Catalytic Triple Bond Activation and Vinyl−Vinyl Reductive Coupling by Pt(IV) Complexes. A Density Functional Study

ARTICLE *in* ORGANOMETALLICS · MARCH 2001

Impact Factor: 4.13 · DOI: 10.1021/om001073u

3 AUTHORS:

Valentine P. Ananikov
Russian Academy of Sciences
141 PUBLICATIONS **2,850** CITATIONS
SEE PROFILE

Djamaladdin G. Musaev
Emory University
277 PUBLICATIONS **8,594** CITATIONS
SEE PROFILE

Keiji Morokuma
Fukui Institute for Fundamental Chemistry
439 PUBLICATIONS **13,611** CITATIONS
SEE PROFILE

Catalytic Triple Bond Activation and Vinyl−Vinyl Reductive Coupling by Pt(IV) Complexes. A Density Functional Study

Valentine P. Ananikov,† Djamaladdin G. Musaev,* and Keiji Morokuma*

Cherry L. Emerson Center for Scientific Computation and Department of Chemistry, Emory University, Atlanta, Georgia 30322

Received December 15, 2000

A density functional theoretical study has been performed for the mechanisms of platinum(IV)-catalyzed alkyne-to-conjugated diene conversion reaction, which involves two subsequent triple bond activation steps followed by vinyl−vinyl coupling. Calculations have shown that acetylene triple bond activation by PtI_6^{2-} in water or methanol solution may proceed through either external nucleophile addition or intramolecular insertion, with the former mechanism occurring with a lower barrier and leading to thermodynamically favored product. The rate-determining step of the entire catalytic cycle is found to be the formation of a platinum(IV) *cis*-divinyl derivative. Although vinyl−vinyl coupling reaction may take place from both six-coordinated octahedral and five-coordinated square-pyramidal platinum(IV) divinyl complexes, the five-coordinated derivative was found to react with a significantly lower barrier. The results obtained here are in good agreement with available experimental data and reveal important details of the catalytic reaction mechanism. The present investigation also has shown that no reliable conclusions may be drawn for the system studied without taking solvent effects into account.

1. Introduction

Transition metal catalyzed C≡C triple bond activation is an important process from the both industrial (conversion of natural alkynes) and synthetic (as a stereo- and regioselective route to unsaturated systems) points of view.[1−3] In general, it involves the C≡C triple bond coordination to a transition metal center, followed by either insertion into a metal−ligand bond or nucleophilic addition.[4−23] Usually, the insertion reaction leads to *cis* products (*cis* with respect to the double bond in metal−vinyl derivatives), while the external nucleophilic attack leads to formation of a *trans* substituted isomer.[10,16,24−32]

Recently, the C≡C bond activation catalyzed by a PtI_6^{2-} complex has been reported,[33−37]

$$PtI_6^{2-} \leftrightarrow PtI_5^- + I^- \quad (1)$$

$$PtI_5^- + C_2H_2 \leftrightarrow [PtI_5(C_2H_2)]^- \quad (2)$$

$$[PtI_5(C_2H_2)]^- + I^- \leftrightarrow [PtI_5(CH{=}CH{-}I)]^{2-} \quad (3)$$

which represents direct reductive coupling of two sp^2-C atoms and is a promising route to synthesis of conjugated dienes with stereodefined geometry. It occurs under room temperature in methanol or water solutions and, in contrast to many other halometalation reactions, produces only *trans* products. The authors proposed a nucleophilic addition pathway as a key activation step. It was demonstrated that for substituted alkynes (HC≡C−CH_2−O−R′) the reaction is also highly regioselective,

† Permanent address: ND Zelinsky Institute of Organic Chemistry, Russian Academy of Sciences, Leninsky Prospect 47, Moscow 117913, Russia.

(1) Collman, J. P.; Hegedus, L. S.; Norton, J. R.; Finke, R. G. *Principles and Application of Organotransition Metal Chemistry*; University Science Books: Mill Valley, CA, 1987.
(2) Crabtree, R. H. *The Organometallic Chemistry of the Transition Metals*; John Wiley & Sons: New York, 1988.
(3) Yamamoto, A. *Organotransition Metal Chemistry*; John Wiley & Sons: New York, 1986.
(4) Musaev, D. G.; Morokuma, K. *Advances in Chemistry and Physics*; Prigogine, I., Rice, S. A., Eds.; John Wiley & Sons: New York, 1996; Vol. XCV, pp 61−127, and references therein.
(5) Koga, N.; Morokuma, K. *Chem. Rev.* **1991**, *91*, 823.
(6) Musaev, D. G.; Morokuma, K. *Top. Catal.* **1999**, *7*, 107.
(7) Anderson, G. K. In *Comprehensive Organometallic Chemistry*; Abel, E. W., Stone, F. G. A., Wilkinson, G., Eds.; Elsevier Science Ltd.; Oxford, 1995; Vol. 9, pp 431−531.
(8) Broene, R. D. In *Comprehensive Organometallic Chemistry*; Abel, E. W., Stone, F. G. A., Wilkinson, G., Eds.; Elsevier Science Ltd.; Oxford, 1995; Vol. 12, pp 323−347.
(9) Elsevier, C. J. *Coord. Chem. Rev.* **1999**, *185−186*, 809.
(10) Bäckvall, J.-E.; Nilsson, Y. I. M.; Gatti, R. G. P. *Organometallics* **1995**, *14*, 4242.
(11) Zagrarian, D.; Alper, H. *Organometallics* **1991**, *10*, 2914.
(12) Garlaschelli, L.; Malatesta, M. C.; Panzeri, S.; Albinati, A.; Ganazzoli, F. *Organometallics* **1987**, *6*, 63.
(13) Huggins, J. M.; Bergman, R. G. *J. Am. Chem. Soc.* **1981**, *103*, 3002.
(14) Maitlis, P. M. *J. Organomet. Chem.* **1980**, *200*, 161.
(15) Otsuka, S.; Nakamura, A. *Adv. Organomet. Chem.* **1976**, *14*, 245.
(16) Chisholm, M. H.; Clark, H. C. *Acc. Chem. Res.* **1973**, *6*, 202.
(17) Cui, Q.; Musaev, D. G.; Morokuma, K. *Organometallics* **1998**, *17*, 1383.
(18) Cui, Q.; Musaev, D. G.; Morokuma, K. *Organometallics* **1998**, *17*, 742.
(19) Cui, Q.; Musaev, D. G.; Morokuma, K. *Organometallics* **1997**, *16*, 1355.
(20) Nakamura, E.; Mori, S.; Nakamura, M.; Morokuma, K. *J. Am. Chem. Soc.* **1997**, *119*, 4887.
(21) de Vaal, P.; Dedieu, A. *J. Organomet. Chem.* **1994**, *478*, 121.
(22) Hada, M.; Tanaka, Y.; Ito, M.; Murakami, M.; Amii, H.; Ito, Y.; Nakatsuji, H. *J. Am. Chem. Soc.* **1994**, *116*, 8754.
(23) Nakamura, E.; Miyachi, Y.; Koga, N.; Morokuma, K. *J. Am. Chem. Soc.* **1992**, *114*, 6686.

10.1021/om001073u CCC: $20.00
Publication on Web 03/21/2001

Scheme 1. Schematic Presentation of the Acetylene Triple Bond Activation and Vinyl−Vinyl Reactions by the Pt^{IV} Complex

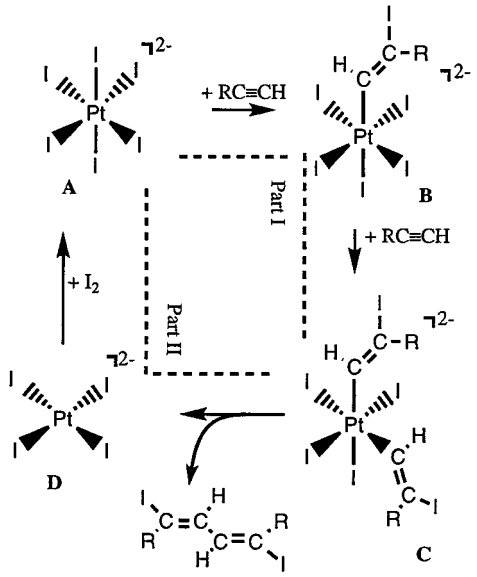

and nucleophilic addition occurs only to the more substituted carbon atom. An intermediate σ-vinyl complex, $[PtI_5(CH{=}CR{-}I)]^{2-}$, **B** (Scheme 1), can be involved in the second triple bond activation step leading to the formation of bis-σ-vinyl derivative $[PtI_4(CH{=}CR{-}I)_2]^{2-}$, **C**. Such derivatives have been isolated and studied using X-ray and NMR methods.[33,34] It has been shown that derivative **C** undergoes a reductive vinyl−vinyl elimination process forming *E*,*E*-1,4-diiodosubstituted dienes as a final product. Note that previously a similar vinyl−vinyl coupling reaction on Ru^{II} [38] and Rh^{III} [39] complexes, as well as reductive elimination of unsaturated ligands between the sp and sp^2 carbon from a Pt^{II} complex has been reported.[40] However, in these cases significant heating is required for reductive elimination, in contrast to a surprising behavior of Pt^{IV} complex **C**, which decomposes at room temperature under the catalytic reaction conditions.[35,37]

The reported catalytic cycle is characterized by surprisingly high stereoselectivity, since in many similar halometalation reactions competing insertion and nucleophilic addition take place under the same reaction conditions[10,25,26,28,30,31] leading to the mixture of isomers and poor stereoselectivity of the activation process. Another interesting feature of this cycle is the usage of Pt^{IV} in the triple bond activation step.[33−37] However, it is generally accepted that Pt^{IV} does not form stable π-complexes,[41,42] with only one exception.[43] Therefore, elucidating the real mechanism and factors effecting the mechanism of this fascinating reaction becomes very interesting. Furthermore, in contrast to the insertion processes, which are known to be key steps in many oligomerization and polymerization reactions,[4−6] activation of unsaturated hydrocarbons through external nucleophilic addition has been theoretically studied less deeply and some of its mechanistic details still remain unclear.

In the present article we report a density functional study of the catalytic cycle mechanism with special attention paid to acetylene triple bond activation and carbon−carbon reductive coupling steps catalyzed by Pt^{IV} iodide complexes (Scheme 2). Here, in addition to the external nucleophilic mechanism originally proposed by experimentalists,[33−37] an alternative mechanism of the alkyne insertion into the Pt−I bond will also be considered. Although theoretical treatment of C−C coupling between sp^3 carbons has been the subject of many papers,[44−48] to the best of our knowledge here we present the first systematic investigation of a vinyl−vinyl reductive elimination reaction. Also, here we report the roles of solvent effects on the reaction mechanisms. Note that previously a similar type of reaction, alkane C−H bond activation, on another halide-rich system (Shilov compound), $[PtCl_4]^{2-}/[PtCl_6]^{2-}$, was experimentally and computationally studied.[49]

2. Calculation Procedure and Reliability Tests

Geometries of the reactants, intermediates, transition states (TSs), and products were optimized using the B3LYP hybrid density functional method.[50−52] Unless otherwise stated, the standard 6-311G(d,p) basis set[53] for C, H, and O and the triple-ζ basis set with the quasi-relativistic energy-adjusted

(24) Hartley, F. R. In *Comprehensive Organometallic Chemistry*; Abel, E. W., Stone, F. G. A., Wilkinson, G., Eds.; Elsevier Science Ltd.; Oxford, 1982; Vol. 6, pp 471−762.
(25) Wang, Z.; Lu, X.; Lei, A.; Zhang, Z. *J. Org. Chem.* **1998**, *63*, 3806.
(26) Dupont, J.; Basso, N. R.; Meneghetti, M. R.; Konrath, R. A.; Burrow, R.; Horner, M. *Organometallics* **1997**, *16*, 2386.
(27) Kataoka, Y.; Matsumoto, O.; Tani, K. *Organometallics* **1996**, *15*, 5246.
(28) Dupont, J.; Casagrande, O. L., Jr.; Aiub, A. C.; Beck, J.; Horner, M.; Bortoluzzi, A. *Polyhedron* **1994**, *13*, 2583.
(29) Murata, T.; Mizobe, Y.; Gao, H.; Ishii, Y.; Wakabayashi, T.; Nakano, F.; Tanase, T.; Yano, S.; Hidai, M.; Echizen, I.; Nanikava, H.; Motomura, S. *J. Am. Chem. Soc.* **1994**, *116*, 3389.
(30) Bäckvall, J. E.; Nilsson, Y. I. M.; Andersson, P. G.; Gatti, R. G. P.; Wu, J. *Tetrahedron Lett.* **1994**, *35*, 5713.
(31) Ma, S.; Lu, X. *J. Org. Chem.* **1991**, *56*, 5120.
(32) Reger, D. L.; Belmore, K. A.; Mintz, E.; McElligott, P. J. *Organometallics* **1984**, *3*, 134, and references therein.
(33) Ananikov, V.; Mitchenko, S. A.; Beletskaya, I. P.; Nefedov, S. E.; Eremenko, I. L. *Inorg. Chem. Commun.* **1998**, *1*, 411.
(34) Ananikov, V.; Mitchenko, S. A.; Beletskaya, I. P. *Dokl. Chem.* **1998**, *363*, 225.
(35) Mitchenko, S. A.; Ananikov V. P.; Beletskaya, I. P.; Ustynyuk, Y. A. *Mendeleev Commun.* **1997**, *4*, 130.
(36) Ananikov V. P.; Mitchenko, S. A.; Beletskaya, I. P. *J. Organomet. Chem.* **2000**, *604*, 290.
(37) Ananikov V. P. Ph.D. Thesis, N.D. Zelinsky Institute of Organic Chemistry, Moscow, 1999.
(38) (a) Burn, J. M.; Fickes, M. G.; Hollander, F. J.; Bergman, R. G. *Organometallics* **1995**, *14*, 137. (b) Chang, J.; Bergman, R. G. *J. Am. Chem. Soc.* **1987**, *109*, 4298.
(39) Wang, Z. Q.; Turner, M. L.; Kunicki, R.; Maitlis, P. M. *J. Organomet. Chem.* **1995**, *488*, C11.
(40) Stang, P. J.; Kowalski, M. H. *J. Am. Chem. Soc.* **1989**, *111*, 3356.
(41) Cotton, F. A.; Wilkinson, G. *Advanced Inorganic Chemistry*; John Wiley & Sons: New York, 1988.
(42) *Comprehensive Organometallic Chemistry*; Abel, E. W., Stone, F. G. A., Wilkinson, G., Eds.; Elsevier Science Ltd.: Oxford, 1995; Vol. 9, p 487.
(43) Jennings, P. W.; Parsons, E. J.; Larsen, R. D. *J. Am. Chem. Soc.* **1985**, *107*, 1793.
(44) Hill, G. S.; Puddephatt, R. *Organometallics* **1998**, *17*, 1478.
(45) Blomberg, M. R. A.; Siegbahn, P. E. M.; Nagashima, U.; Wennerberg, J. *J. Am. Chem. Soc.* **1991**, *113*, 424.
(46) Low, J. J.; Goddard, W. A., III. *J. Am. Chem. Soc.* **1986**, *108*, 6115.
(47) Low, J. J.; Goddard, W. W., III. *Organometallics* **1986**, *5*, 609.
(48) Tatsumi, K.; Hoffmann, R.; Yamamoto, A.; Stille, J. K. *Bull. Chem. Soc. Jpn.* **1981**, *54*, 1857.
(49) (a) Stahl, S. S.; Labinger, J. A.; Bercaw, J. E. *Angew. Chem., Int. Ed.* **1998**, *37*, 2180. (b) Siegbahn, P. E. M.; Grabtree, R. H. *J. Am. Chem. Soc.* **1996**, *118*, 4442.
(50) Becke, A. D. *Phys. Rev. A* **1988**, *38*, 3098.
(51) Lee, C.; Yang, W.; Parr, R. G. *Phys. Rev. B* **1988**, *37*, 785.
(52) Becke, A. D. *J. Chem. Phys.* **1993**, *98*, 5648.

Scheme 2. CC Triple Bond Activation Mechanisms

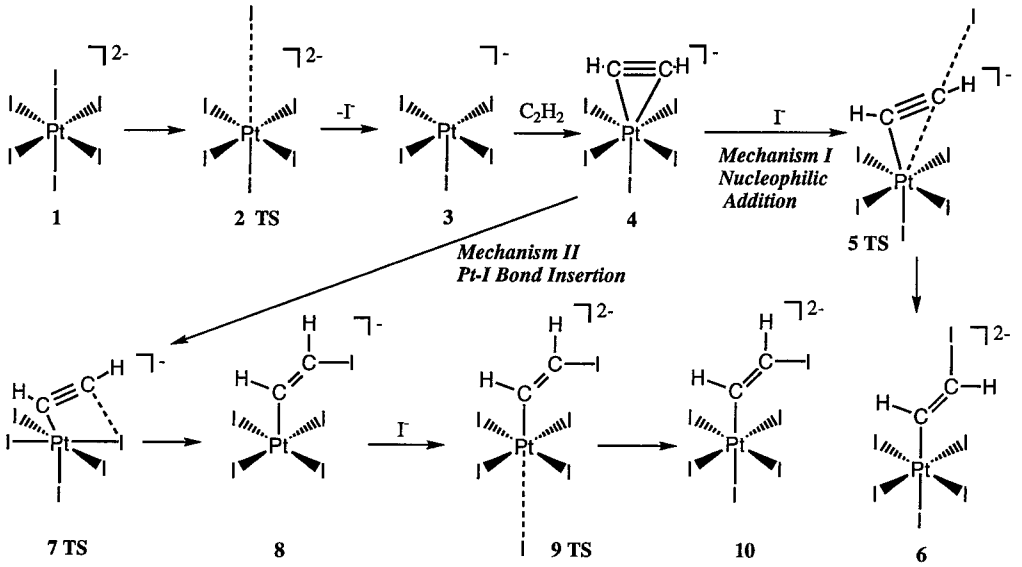

spin−orbit-averaged Stuttgart/Dresden effective core potentials (ECP) for iodine and Pt[54−57] were used in these calculations (BSI). The Stuttgart/Dresden ECPs used in this paper have shown very good performance in various systems.[54,57−61] Normal coordinate analysis has been performed for all stationary points to characterize the TSs (one imaginary frequency) and equilibrium structures (no imaginary frequencies) and to calculate zero-point energy correction (ZPC) and Gibbs free energies (at 298.15 K, 1 atm). In the most important cases IRC calculations near the TS region followed by geometry optimization of both reactants and products were performed to confirm the connectivity of the TSs (further referred to as IRC).

The solvent effect has been studied using the polarized-continuum-model (PCM) approximation.[62−68] The PCM-B3LYP/BSI energy calculations have been performed at the B3LYP/BSI optimized geometries. In other words, we did not reoptimize the structures in the presence of solvent since previously it has been shown that reoptimization of the geometry has very limited effect on the computed solvation energies.[69−73] All PCM calculations were carried out at 298.15 K using an average tesserae area[70] of 0.4 Å^2. All calculations were carried out using the Gaussian98 program.[74]

Table 1. Calculated and Experimental Pt−I Bond Lengths (in Å)

method[a]	PtI_4^{2-}	PtI_6^{2-}
B3LYP/BSI	2.764	2.800
B3LYP/SDD(d)[b]	2.743	2.789
B3LYP/SDD(2d,2f)[c]	2.732	2.779
B3LYP/SDD+(df)[d]	2.720	2.770
experimental	2.61[e]	2.673[f]

[a] Stuttgart/Dresden valence and ECP basis set for Pt[56] and, unless otherwise noted, Stuttgart/Dresden valence and ECP basis set for I[54,55,57] were used in all cases, and the polarization and diffuse functions were added to iodine atoms only. [b] Modified valence basis set[55] with additional d-polarization function (exponent 0.266). [c] Modified valence basis set[55] supplemented with d- and f-polarization functions according to ref 92. [d] Augmented with polarization and diffuse (exponents of 0.0591(s) and 0.0333(p)) functions according to ref 59. [e] $K_2[PtI_4]\cdot 2H_2O$ structure.[79] [f] $Cs_2[PtI_6]$ structure.[80]

To test the reliability of the approximations used in this paper, we have performed four different tests. First, we have calculated Pt−I bond distances for the PtI_2, PtI_4^{2-}, and PtI_6^{2-} complexes at the B3LYP/BSI level and compared those with available experimental (X-ray) data (see Table 1). For the neutral PtI_2, the calculated Pt−I distance, 2.559 Å, agrees well with experimental observations, 2.58−2.60 Å.[75] However, for the anionic PtI_4^{2-} and PtI_6^{2-} complexes the calculated Pt−I bond lengths are 0.13−0.15 Å longer than experimental values. An extensive study for both complexes (Table 1) has shown

(53) Krishnan R.; Binkley, J. S.; Seeger, R.; Pople, J. A. *J. Chem. Phys.* **1980**, *72*, 650.
(54) Schwerdtfeger, P.; Dolg M.; Schwarz, W. H.; Bowmaker, G. A.; Boyd, P. D. W. *J. Chem. Phys.* **1989**, *91*, 1762.
(55) Dolg. M. Ph.D. Thesis, Universitat Stuttgart, 1989.
(56) Andrae, D.; Haubermann, U.; Dolg, M.; Stoll, H.; Preub, H. *Theor. Chim. Acta* **1990**, *77*, 123.
(57) Bergner, A.; Dolg M.; KŸchle, W.; Stoll, H.; Preuss, H. *Mol. Phys.* **1993**, *80*, 1431.
(58) Dolg, M. *Mol. Phys.* **1996**, *88*, 1645.
(59) Glukhovtsev, M. H.; Pross, A.; McGrath, M. P.; Radom, L. *J. Chem. Phys.* **1995**, *103*, 1878.
(60) Kaupp, M.; v. Schnering, H. G. *Inorg. Chem.* **1994**, *33*, 2555.
(61) El-Nahas, A. M.; Schleyer, P. v. R. *J. Comput. Chem.* **1994**, *15*, 596.
(62) Cossi, M.; Barone, V.; Cammi, R.; Tomasi, J. *Chem. Phys. Lett.* **1996**, *255*, 327.
(63) Fortunelli, A.; Tomasi, J. *Chem. Phys. Lett.* **1994**, *231*, 34.
(64) Tomasi, J.; Persico, M. *Chem. Rev.* **1994**, *94*, 2027.
(65) Floris, F.; Tomasi, J. *J. Comput. Chem.* **1989**, *10*, 616.
(66) Pascual-Ahuir, J. L.; Silla, E.; Tomasi, J.; Bonaccorsi, R. J. *J. Comput. Chem.* **1987**, *8*, 778.
(67) Mieritus, S.; Tomasi, J. *J. Chem. Phys.* **1982**, *65*, 239.
(68) Mieritus, S.; Scrocco, E.; Tomasi, E. *J. Chem. Phys.* **1981**, *55*, 117.
(69) Barone, V.; Cossi, M.; Tomasi, J. *J. Chem. Phys.* **1997**, *107*, 3210.
(70) Pomeli, C. S.; Tomasi, J.; Sola, M. *Organometallics* **1998**, *17*, 3164.
(71) Cacelli, I.; Ferretti, A. *J. Chem. Phys.* **1998**, *109*, 8583.
(72) Creve, S.; Oevering, H.; Coussens, B. B. *Organometallics* **1999**, *18*, 1907.
(73) Bernardi, F.; Bottoni, A.; Miscone, G. P. *Organometallics* **1998**, *17*, 16.
(74) Frisch, M. J.; Trucks, G. W.; Schlegel, H. B.; Scuseria, G. E.; Robb, M. A.; Cheeseman, J. R.; Zakrzewski, V. G.; Montgomery, J. A., Jr.; Stratmann, R. E.; Burant, J. C.; Dapprich, S.; Millam, J. M.; Daniels, A. D.; Kudin, K. N.; Strain, M. C.; Farkas, O.; Tomasi, J.; Barone, V.; Cossi, M.; Cammi, R.; Mennucci, B.; Pomelli, C.; Adamo, C.; Clifford, S.; Ochterski, J.; Petersson, G. A.; Ayala, P. Y.; Cui, Q.; Morokuma, K.; Malick, D. K.; Rabuck, A. D.; Raghavachari, K.; Foresman, J. B.; Cioslowski, J.; Ortiz, J. V.; Baboul, A. G.; Stefanov, B. B.; Liu, G.; Liashenko, A.; Piskorz, P.; Komaromi, I.; Gomperts, R.; Martin, R. L.; Fox, D. J.; Keith, T.; Al-Laham, M. A.; Peng, C. Y.; Nanayakkara, A.; Gonzalez, C.; Challacombe, M.; Gill, P. M. W.; Johnson, B.; Chen, W.; Wong, M. W.; Andres, J. L.; Gonzalez, C.; Head-Gordon, M.; Replogle, E. S.; Pople, J. A. *Gaussian 98*, Revision A.7; Gaussian, Inc.: Pittsburgh, PA, 1998.
(75) Thiele, G.; Weigl, W.; Wochner, H. *Z. Anorg. Allg. Chem.* **1986**, *539*, 141.

Scheme 3. Activation of the Second Acetylene Molecule by Pt^{IV} Vinyl Complexes, 6

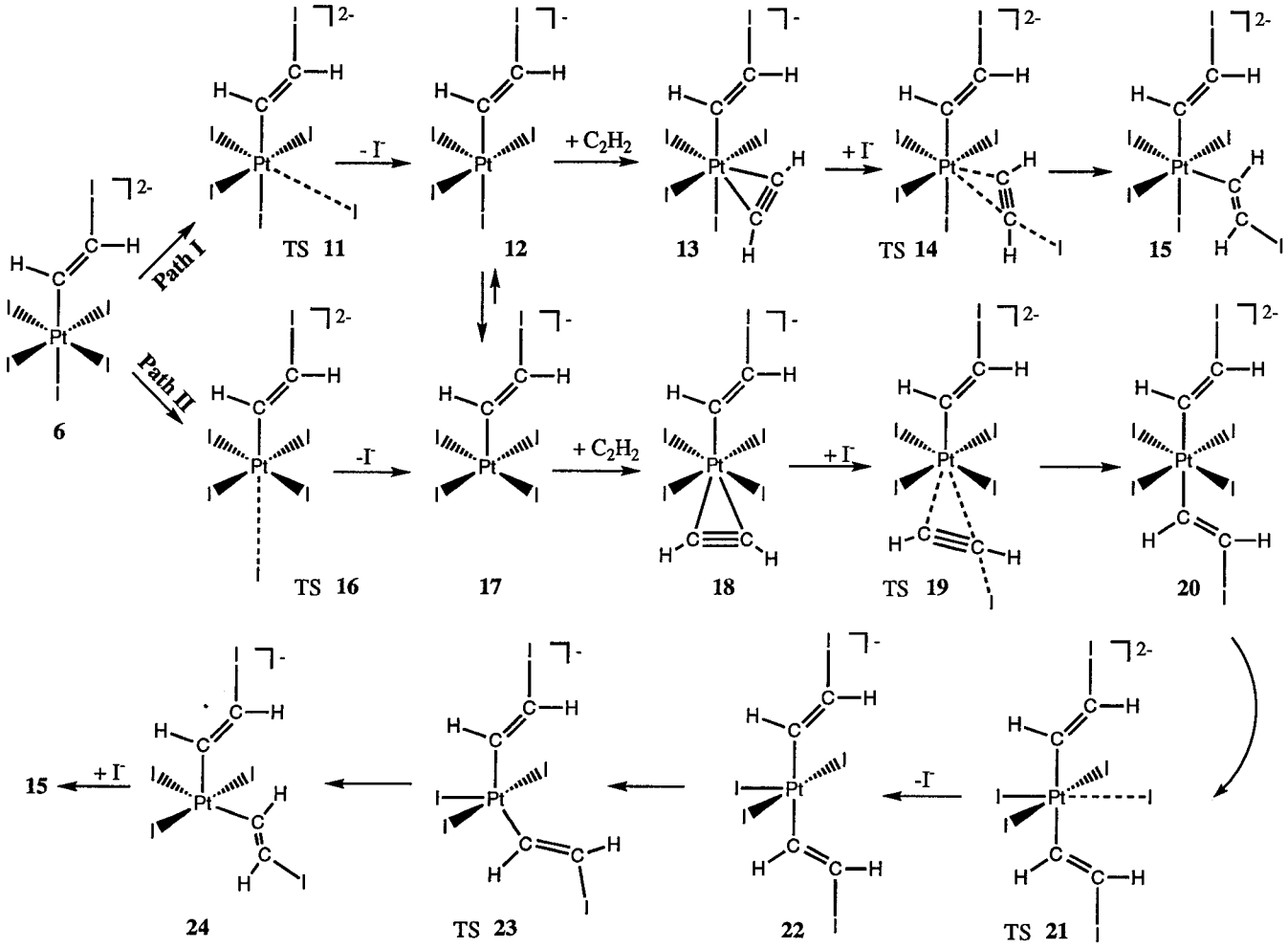

that this discrepancy between experimental and calculated values is not due to the basis sets adopted, since even with the large iodine basis set supplemented with d-, f- and diffuse sp-shell functions the calculated Pt−I bonds are still 0.1 Å longer than experiment. We believe that the difference between calculated and experimental values of the Pt−I bonds of anionic PtI_4^{2-} and PtI_6^{2-} complexes is a result of the absence of the contour-ion effects in the calculations.[76−78] The β-PtI_2 crystal,[75] from which the experimental value was taken, consists of approximately square-planar PtI_4 units linked through iodine atoms, in the $K_2[PtI_4]\cdot 2H_2O$ salt,[79] where the Pt···K distance is quite short, 3.44 Å. Similarly, in the platinum(IV) iodide (Cs_2PtI_6)[80] the Cs atoms are located at a distance of 4.02 Å from I. A detailed consideration of these questions is out of the scope of the current article.

Second, we have performed the B3LYP/BSI geometry optimization of the key intermediate complex [Pt(CH═CI−CH_2-OCH_3)$_2$$I_2$] (with C_s-symmetry constraint), for which the experimental structure is known.[33] An average deviation of 0.017 Å for bond lengths and 0.8° for bond angles were obtained between optimized and experimental structures. Furthermore, one of the most important parameters, the Pt−C σ-bond length, has been obtained with an excellent accuracy, with the calculated value of 2.004 Å vs experimental, 1.994(14) and 1.995(16) Å. Third, we have calculated the energy difference between low-lying $^3D(s^1d^9)$ and $^1S(s^0d^{10})$ electronic states of a single platinum atom. The calculations correctly reproduce ^3D-(s^1d^9) as a ground state and $^1S(s^0d^{10})$ being 9.2 kcal/mol higher in energy. The experimental energy difference is 11.1 kcal/mol,[81] from which the calculated value deviates by less than 2 kcal/mol, confirming a good accuracy of the theoretical method used. The conclusion is in line with the results obtained earlier.[19,82]

Fourth, we have calculated the free energy of hydration for the iodide ion using the PCM method. The PCM-B3LYP/BSI method used in this paper gave a value of 63.6 kcal/mol, which is in a good agreement with the experimental 61 ± 2 kcal/mol.[83] No significant basis set effects on the free energy of hydration were found; that is, at the PCM-B3LYP/SDD+(df) level (see footnote of Table 1 for the basis set description) the calculated value was 63.9 kcal/mol. On the basis of the benchmark results above, we believe that the chosen theoretical methods are adequate for study of the above-presented problems.

Below, in our discussions, we will divide the reaction into two parts. Part I, the catalytic alkyne conversion part, includes (a) activation of the catalyst, (b) alkyne coordination to the Pt complex, (c) conversion of the coordinated alkyne to haloalkene, and (d) coordination of the second alkyne molecule and its conversion. In part II, the reductive vinyl−vinyl elimination

(76) Danzeisen, O.; Rotter, H. W.; Thiele, G. *Z. Anorg. Allg. Chem.* **1998**, *624*, 763.
(77) Baechle, W.; Rotter, H. W.; Thiele, G.; Clark, R. J. H. *Inorg. Chim. Acta* **1992**, *191*, 121.
(78) Brodersen, V. K.; Thiele, G.; Holle, B. *Z. Anorg. Allg. Chem.* **1969**, *369*, 155.
(79) Ollson, L.-F.; Oskarsson, A. *Acta Chim. Scand.* **1989**, *43*, 811.
(80) Sinram, D.; Brendel, C.; Krebs, B. *Inorg. Chim. Acta* **1982**, *64*, L131.
(81) Moore, C. F. *Atomic Energy Levels*, NSRD-NBS.; U.S. Goverment Printing Office: Washington, DC, 1971; Vol. III.
(82) Musaev, D. G.; Morokuma, K. *J. Phys. Chem.* **1996**, *100*, 6509.
(83) Pearson, R. G. *J. Am. Chem. Soc.* **1986**, *108*, 6109.

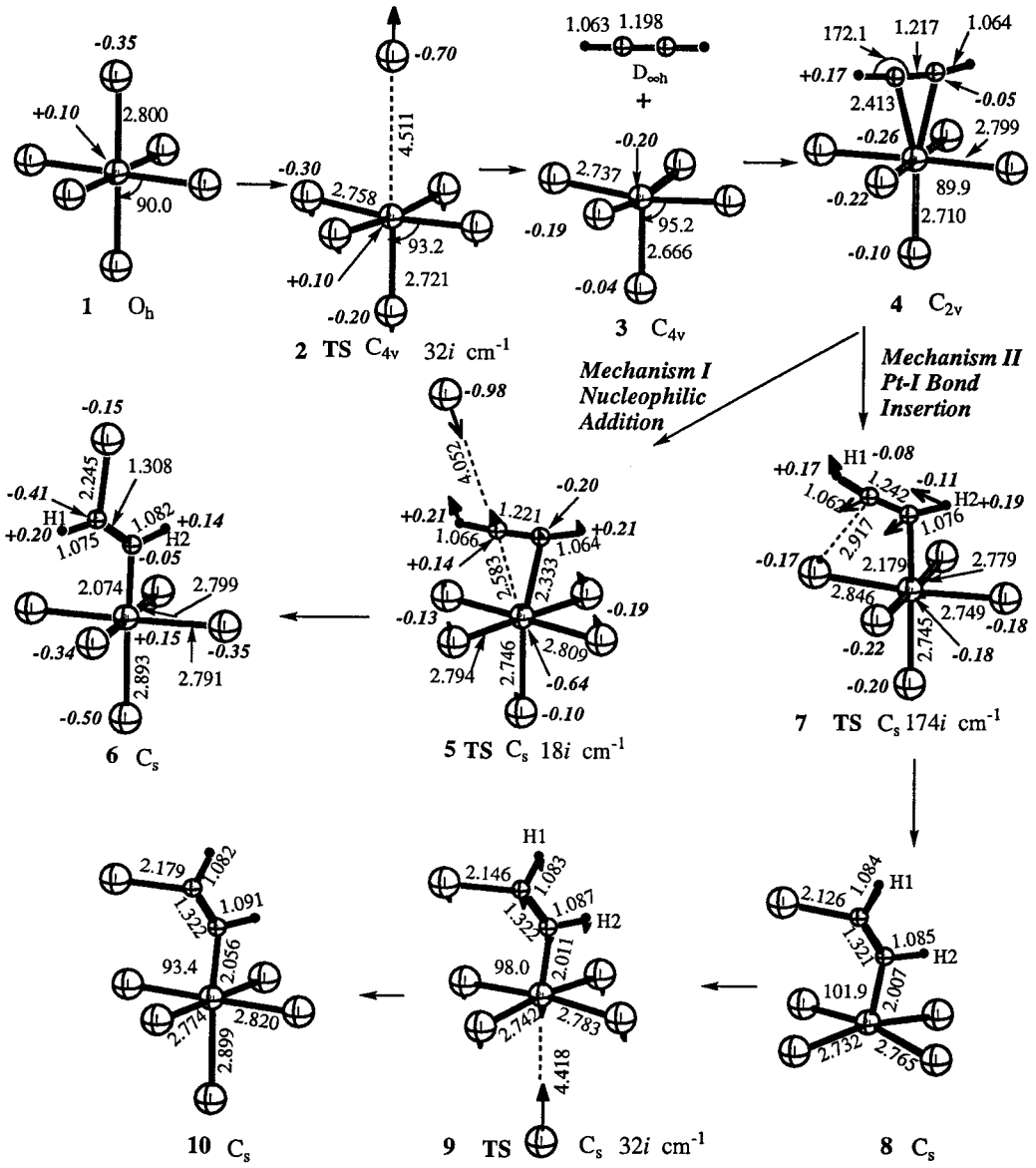

Figure 1. B3LYP/BSI optimized geometries (in Å and deg) and Mulliken charges (in bold italic) of the reactants, intermediates, TSs, and products of the acetylene coordination and activation reactions.

process, we will mainly discuss the reductive vinyl−vinyl elimination process forming *E*,*E*-1,4-diiodosubstituted dienes as a final products.

Although we have calculated the zero-point energy corrections (ZPC) and Gibbs free energies (ΔG) for all compounds, below we will mainly discuss the B3LYP energy (ΔE). However, at the end of each section of the paper will be given a comparative discussion of these values, ZPEC and ΔG, with ΔE. This strategy allows us to highlight the question of accuracy in details and develop adequate methodology in view of possible future investigations of large catalytic systems.

3. The Mechanism of Catalytic Alkyne Conversion Reactions

This section is divided into two subsections. Subsection A deals with the gas-phase calculations, whereas the solvent effects are described in subsection B. In both subsections, the following stages are discussed: (i) C≡C triple bond activation via both the nucleophilic addition and the Pt−I insertion leading to a Pt(IV) σ-vinyl complex (Scheme 2) and (ii) the second acetylene molecule activation by the Pt(IV) σ-vinyl complex leading to a bis(vinyl)Pt(IV) complex (Scheme 3). Optimized structures and selected geometry parameters are shown in Figures 1 and 2, and their relative energies are summarized in Table 2 and Figure 3.

A. Gas-Phase Calculations. Dissociation of the Initial Pt(IV) Iodide Complex and Acetylene Coordination and Activation. The first step of the proposed mechanism for the C≡C triple bond activation (see Scheme 2) is the I^- ligand dissociation from the initial octahedral PtI_6^{2-} complex, **1** (see also Figure 1). The TS **2** for the dissociation has been located at a distance of 4.511 Å between Pt and the leaving iodide ligand. Normal-mode analysis shows that the structure has only one imaginary frequency of 32i cm^{-1}. The normal mode visualization as well as IRC calculations confirm that TS **2** connects reactant **1** to products of this dissociation step, **3** + I^-. In this TS all Pt−I distances are significantly shorter than in the reactant **1**; the Pt−I bond in *trans* position to the leaving ligand is 0.037 Å shorter than corresponding bonds in *cis* orientation, indicating weakening of the *trans* influence. The same

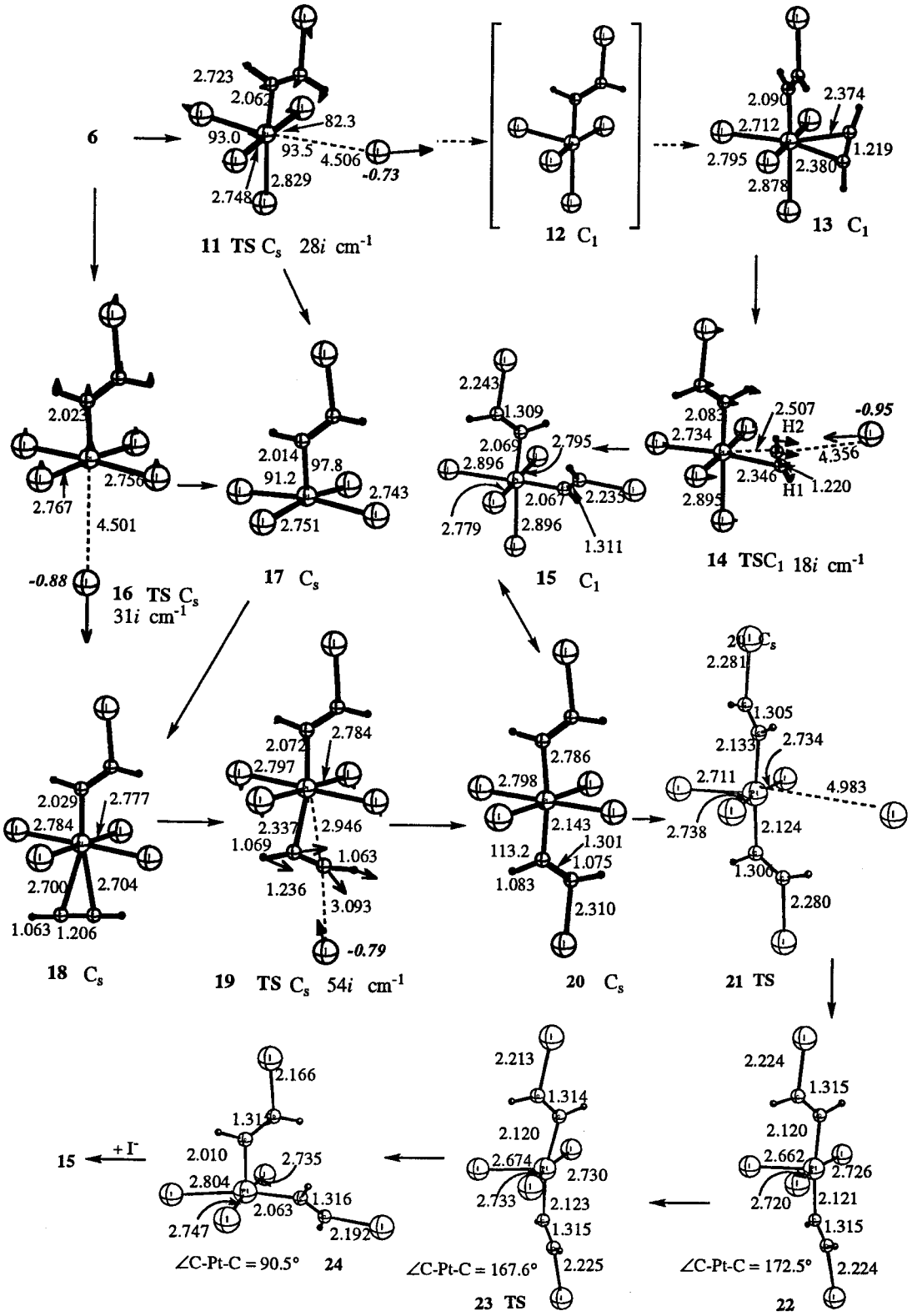

Figure 2. B3LYP/BSI optimized geometries (distances in Å, and angles in deg) of the reactants, intermediates, TSs, and products of the second acetylene activation by the Pt^{IV} vinyl complex, **6**.

tendency is observed upon going from TS **2** to product **3**; the difference between axial and equatorial Pt−I distances increases to 0.071 Å and gives the geometry that is typically expected for the square pyramidal complexes.[1,84] The activation energy is calculated to be 18.1 kcal/mol relative to complex **1**, and reaction **1** → **3** + I^- is found to be exothermic by 30.3 kcal/mol (see Table 2). The Mulliken analysis shows that iodine atoms are negatively charged in all complexes **1**−**3**. In addition, the charge on the leaving iodide ligand, −0.70 e, confirms the heterolytic nature of the dissociation process.

It should be noted that in the case of five-coordinated

(84) Hoffmann, R. *Angew. Chem., Int. Ed. Engl.* **1982**, *21*, 711.

Table 2. Calculated Relative Energies (Δ*E*) and Free Energies (Δ*G*) in the Gas Phase and in Aqueous and Methanol Solutions of Reactants, Intermediates, TSs, and Products (in kcal/mol)[a,b]

	gas phase			PCM-water		PCM-methanol	
structure	ΔE	ΔE+ZPC	ΔG	$\Delta E_{solution}$	$\Delta G_{solution}$	$\Delta E_{solution}$	$\Delta G_{solution}$
1	0.0	0.0	0.0	0.0	0.0	0.0	0.0
2	18.1	17.8	17.5	20.5	23.7	20.6	22.8
3	−30.3	−30.5	−38.0	13.4	11.5	11.9	9.8
4	−34.3	−33.4	−30.9	8.9	5.2	7.4	4.6
5	0.0	0.8	9.0	14.0	14.5	13.6	14.1
6	−15.1	−12.7	−3.3	−7.3	−7.9	−7.6	−7.7
7	−25.8	−25.5	−23.0	16.1	12.8	14.7	12.1
8	−44.4	−42.1	−40.7	−0.7	−4.2	−2.1	−5.0
9	8.6	10.9	19.9	9.5	11.4	9.5	11.2
10	−2.6	−0.1	9.8	0.4	−0.8	0.1	−0.4
11	2.5	4.6	13.2	14.7	17.8	14.3	16.9
12	−41.1	−38.8	−37.9	5.1	2.2	9.0	6.8
13	−46.5	−42.8	−31.1	−2.2	−6.7	−3.6	−6.7
14	−13.3	−10.0	7.8	6.9	6.5	6.8	7.1
15	−30.1	−25.2	−6.4	−14.7	−16.0	−15.4	−15.6
16	−2.8	−0.5	7.9	3.8	6.2	3.7	5.7
17	−53.3	−51.0	−49.7	−6.7	−9.6	−8.2	−10.6
18	−55.9	−52.3	−41.2	−8.4	−12.2	−10.0	−12.5
19	−17.1	−13.9	4.6	4.9	3.8	3.9	3.7
20	−21.5	−17.2	1.2	−3.6	−5.2	−4.2	−4.6
21	0.6	4.5	21.2	18.7	20.4	18.9	20.7
22	−40.3	−36.0	−26.2	11.6	7.4	9.8	6.7
23	−40.2	−36.0	−24.5	10.8	6.8	9.1	6.2
24	−64.0	−59.1	−48.3	−15.5	−19.3	−17.2	−20.0
25	−30.6	−25.7	−6.4	−15.8	−16.8	−16.5	−16.5
26	−2.6	2.0	21.2	4.3	3.9	3.8	4.3
27	−37.1	−31.0	−23.7	−48.1	−53.5	−48.2	−52.6
28	−28.9	−24.1	−4.2	−15.2	−16.3	−15.6	−15.7
29	2.5	7.0	25.8	10.3	10.0	10.0	10.5
30	−33.9	−27.9	−20.6	−44.5	−49.9	−44.6	−48.9
31	−63.2	−58.4	−47.6	−14.6	−18.2	−16.3	−18.9
32	−55.4	−50.3	−38.4	−7.6	−11.9	−9.2	−12.3
33	−94.3	−87.2	−75.6	−49.5	−54.1	−50.9	−54.3
34	−61.6	−56.9	−45.4	−13.3	−17.1	−14.9	−17.7
35	−52.2	−47.1	−35.3	−6.7	−11.1	−8.2	−11.4
36	−90.7	−83.7	−72.3	−46.7	−51.1	−48.1	−51.3

[a] Energies were calculated relative to structure **1**. The total energies (in au) of **1** are as follows: in gas phase, $\Delta E = -342.919275$, ΔE + ZPC = −342.862066, $\Delta G = -342.950866$; in PCM-water, $\Delta E_{solution} = -343.1581689$, $\Delta G_{solution} = -343.139656$; in PCM-methanol: $\Delta E_{solution} = -343.1522457$, $\Delta G_{solution} = -343.147445$. [b] Geometries of all compounds were optimized at the B3LYP/BSI level; in geometry optimization of point **12** the C−Pt−I_{trans} angle was constrained at 176.2°, the optimized value for **6** (see text for details).

complex, in principle, a trigonal bipyramidal structure could be considered as an alternative for the square pyramidal structure. However, we found that PtI_5^- in the trigonal bipyramidal structure is unstable and converges to the square pyramidal form without a barrier during geometry optimization. Therefore, this type of complex will not be considered.

Starting from complex **3**, the next step is acetylene coordination leading to the formation of the π-complex **4**. This step is calculated to be 4.0 kcal/mol exothermic (see Table 2), but the entropy contribution makes **4** less stable than **3**. The small calculated binding energy is consistent with the relatively long Pt−C distance (2.413 Å) and insignificant geometry distortions of coordinated acetylene; the C≡C bond is elongated by 0.019 Å and the H−C≡C angle is decreased by 8° in complex **4** compared with those in the free acetylene molecule. Complex **4** can be considered as a very weakly bound π-complex, which most likely cannot be isolated. The calculated small stability of **4** can be attributed to a small back-donation ability of platinum in high oxidation state and a strong exchange repulsion between the acetylene π-system and bulky iodide ligands. Similar conclusions have been drawn in the case of weak bonding of acetylene with the Pd complex.[21] The HC≡CH ligand is staggered with respect to the equatorial Pt−I bonds, to avoid unfavorable exchange repulsion from them. However, acetylene rotates around the Pt−X axes, where X is the center of C≡C bond, with a barrier of 2.2 kcal/mol (see Figure S1 in the Supporting Information). The above presented results are in a good agreement with experimental findings, confirming that no Pt^{IV}-π-complex exists, with rare exceptions.[41−43]

From complex **4**, the reaction may proceed via two different mechanisms, as shown in Scheme 2. Mechanism I corresponding to the nucleophilic addition of the dissociated I^- to the coordinated acetylene occurs via TS **5**, where the PtI_5 fragment is slipped by 0.093 Å from the center of the C≡C bond (see Scheme S1 in the Supporting Information). The slippage results in asymmetrical acetylene binding: one of the platinum−carbon bonds is 0.170 Å longer, while the second Pt−C distance is 0.080 Å shorter as compared to the η^2-structure **4**. A geometry change toward a η^1-type of structure also increases the Pt−C−C angle from 75.4° in **4** to 87.4° in **5**. As a result of these changes, the positive charge on the carbon atom being attacked by the I^- increases to +0.14 e. A relatively long I−C distance (4.052 Å) and a large negative charge on the incoming iodide (−0.99 e) indicate that the TS is more reactant-like. The normal-mode analysis gives an unusually small imaginary frequency, 18i cm^{-1}. The IRC calculations in both

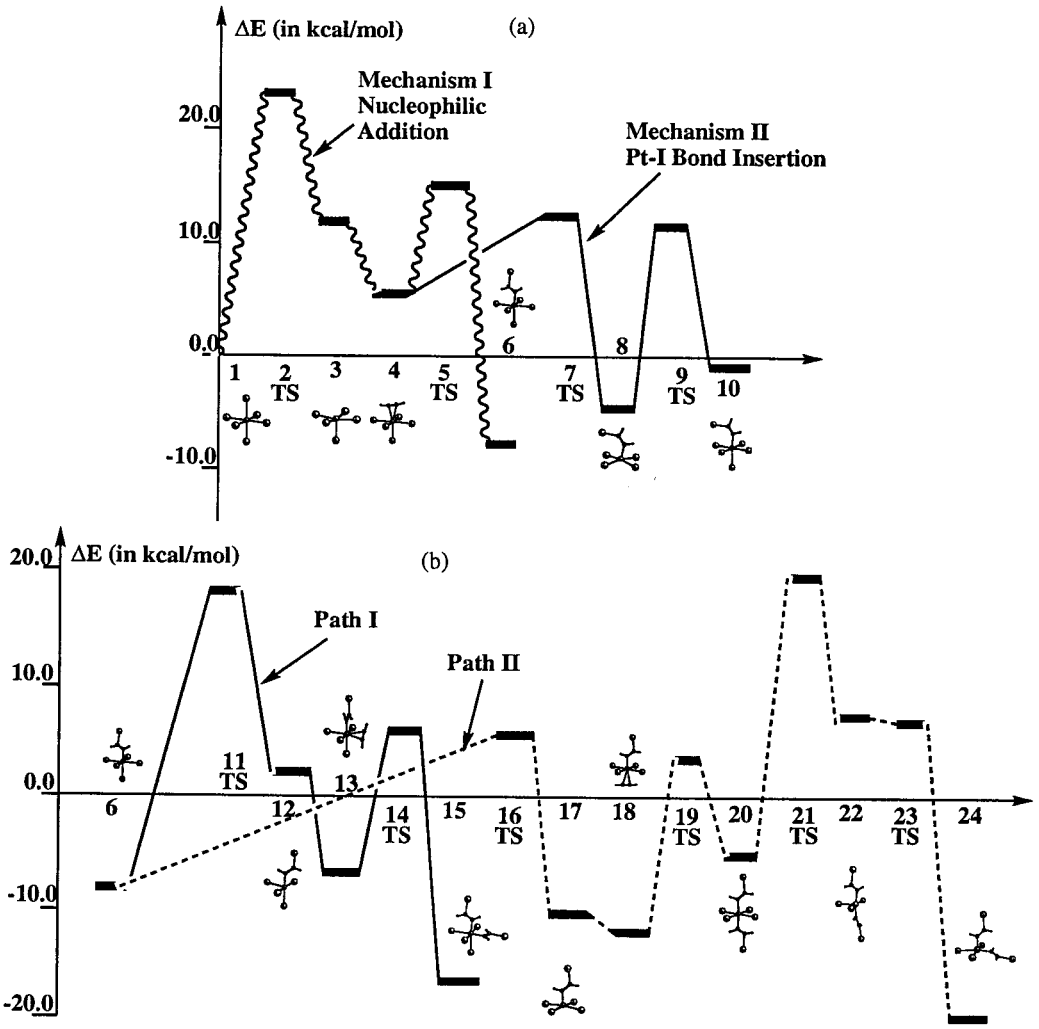

Figure 3. Potential energy profiles of the reactions of the (a) first and (b) second acetylene activation by Pt^{IV} complexes, presented using $\Delta G_{solution}$ in the aqueous solution (see Table 2).

reactant and product directions confirm that TS **5** connects **4** with **6**.

Overcoming the TS **5** leads to the formation of *trans*-σ-vinyl complex **6**, where both carbon atoms possess geometrical parameters typical for sp^2 hybridization. The Pt−I bond *trans* to the carbon atom is 0.1 Å longer compared to those in the *cis* position, confirming the high *trans* influence of the σ-vinyl ligand.[85] Complex **6** also has a staggered Pt−C bond; the barrier of rotation around the Pt−C bond is calculated to be less than 1 kcal/mol (see Figure S1 in the Supporting Information). Since the gas-phase reaction **4** → **5** → **6** is calculated to be endothermic by 19.2 kcal/mol and proceeds with a high (34.3 kcal/mol) barrier at the TS **5** (see Table 2), one may conclude that the triple bond activation via this mechanism is impossible at room temperature. This conclusion contradicts the available experimental observations.[35]

The alternative acetylene activation mechanism, mechanism II, corresponds to the insertion of the coordinated acetylene molecule into the Pt−I bond, which occurs via the TS **7**, as shown in Figure 1. The C_2H_2 group in the insertion TS **7** is much closer to the metal than in the nucleophilic addition TS **5**; the Pt−C distance is 2.179 Å in **7** vs 2.333 Å in **5**. The same tendency is also found in the forming carbon−iodine bond, 2.917 Å in **7** vs 4.052 Å in **5**. Normal-mode analysis shows that structure **7** has only one imaginary frequency, 174i cm^{-1}. The activation energy starting from π-complex **4** is calculated to be 8.5 kcal/mol. The product of the reaction, complex **8**, was found to be 10.1 kcal/mol lower in energy than reactant **4**.

In the next step complex **8** can coordinate one iodide ligand to form structure **10** through the TS **9**. Geometry changes during the reaction path **8** → **9** → **10** reflect further increase in the steric strain. Due to interaction of *cis*-iodide ligands with the incoming ligand, the angle *cis*-I−Pt−C is decreased from 101.9° in **8** to 98.0° in the TS and, finally, to 93.4° in the product. To compensate introduced repulsion, the Pt−C−C angle has to be increased by 7.7° from **8** to **10**. Formation of **10** is highly endothermic, 41.8 kcal/mol compared to **8**, reflecting the increased instability caused by interaction between the iodo-vinyl and iodide ligands, as described above. The large activation energy, 53.0 kcal/mol, at the TS **9**, combined with high endothermicity, makes the reaction **8** → **9** → **10** impossible under mild conditions.

As a result of the insertion reaction, the product **8** with *cis*-(Z) orientation is formed, in contrast to the

(85) Anderson, G. K. In *Comprehensive Organometallic Chemistry*; Abel, E. W., Stone, F. G. A., Wilkinson, G., Eds.; Elsevier Science Ltd.: Oxford, 1995; Vol. 9, p 487.

trans-σ-vinyl product **6** formed via the nucleophilic addition reaction. A comparison of both activation mechanisms, presented above, shows that in the gas phase acetylene insertion into the Pt−I bond (mechanism II) to form complex **9** is easier than nucleophilic addition leading to **6**. However, as mentioned above, the formation of the *cis*-(Z) species has not been observed under the experimental conditions.[33−37] Thus, our findings do not agree with the available experiment. Despite this, we will continue our detailed studies of mechanism I, since only this reaction pathway will give a final product with the desired stereoselectivity.

As shown in Table 2, ZPC on the first iodide ligand dissociation step and the activation energy for both insertion and nucleophilic addition mechanisms are very small. The calculated acetylene binding energy, 4.0 kcal/mol, decreases by 1.1 kcal/mol upon including ZPC to 2.9 kcal/mol.

Meantime, upon comparing gas-phase energies and gas-phase Gibbs free energies presented in Table 2, one may find rather small differences, except for the bond dissociation and bond formation steps. Indeed, $\Delta G^{\ddagger}$ and ΔG of the iodide dissociation step decrease to 17.5 and −38.0 kcal/mol, compared to $\Delta E^{\ddagger}$ and ΔE values of 18.1 and −30.3 kcal/mol, thus facilitating the process. The Gibbs free energy of acetylene triple bond activation via insertion mechanism (**4** → **7** → **8**) does not deviate significantly from the relative energy. However, the entropy contribution to triple bond activation reaction via external nucleophilic addition (**4** → **5** → **6**) cannot be neglected, where $\Delta G^{\ddagger} = 39.9$ kcal/mol and $\Delta G = 27.6$ kcal/mol compared with $\Delta E^{\ddagger} = 34.3$ kcal/mol and $\Delta E =$ 19.2 kcal/mol, respectively. Thus, inclusion of the entropy effects makes this type of triple bond activation absolutely impossible under mild conditions, in contrast to experimental findings. Also, it is interesting to note that π-complex formation (**3** → **4**) becomes endothermic, $\Delta G = 7.1$ kcal/mol upon including the entropy effects (vs $\Delta E = -4.0$ kcal/mol), confirming the unstable nature of this intermediate **4**.

Activation of the Second Acetylene Molecule. As we have shown earlier, the triple bond activation reaction has to be started with the iodine dissociation step followed by alkyne coordination. For complex **6**, which is a starting structure for the second acetylene addition reaction, there are two possible dissociation pathways (see Scheme 3), **path I** and II, corresponding to the *cis* and *trans* iodine ligand dissociation, respectively. Let us to discuss these paths separately in detail.

As shown Figure 2, in path I, dissociation of an iodide ligand *cis* to the CH═CHI group occurs through the TS **11**, which has eclipsed conformation, i.e., the C═C axis lies in the same plane with the breaking Pt−I bond. The TS structure is similar to **2**, has one imaginary frequency of 28i cm^{-1}, and is 17.6 kcal/mol above the reactant **6**. It is natural to expect that overcoming the barrier at TS **11** will lead to structure **12**. However, surprisingly, we were not able to find a stationary point corresponding to complex **12**; it converged to complex **17** without any energetic barrier during geometry optimization.

Interestingly, if a structure like **12** existed, the next step of reaction could be addition of the acetylene molecule to form the π-complex **13**. Although formation of π-complex **13** from **12** is impossible because structure **12** with a coordination vacancy is not a stationary point, it is interesting to examine whether the second iodoplatination of acetylene can take place. The optimized structure of mixed π,σ-complex **13** is shown in Figure 2. The Pt−I bond lengths located *trans* to the CH═CHI, I, and C_2H_2 ligands are 2.878, 2.795, and 2.712 Å, respectively. Point **12**, obtained by optimization with the constraint of the $C-Pt-I_{trans}$ angle at 176.2° (the optimized value for **6**), is calculated to be 5.4 kcal/mol higher in energy than the mixed *cis*-π,σ-complex **13**. Starting from complex **13**, the triple bond activation process takes place via the TS **14**. Normal-mode analysis gives only one imaginary frequency of 18i cm^{-1} for this TS. Visualization of the corresponding vibration and IRC calculations clearly shows that this TS connects **13** to **15**. Compared to the first triple bond activation TS **5**, **14** is more reactant-like, the forming I−C distance is longer (4.356 Å in **14** vs 4.052 Å in **5**), and the difference in breaking and forming Pt−C bonds in **14** (2.507 − 2.346 = 0.161 Å) is smaller than that in **5** (2.583 − 2.333 = 0.250 Å). The activation energy required to break the triple bond starting from π-complex **13** is calculated to be 33.2 kcal/mol. Overcoming TS **14** leads to the formation of *cis*-divinyl complex **15**. The process **13** → **14** → **15** is found to be endothermic by 16.4 kcal/mol.

Path II starts with dissociation of the *trans* iodide ligand from complex **6**, which occurs through the TS **16**. The calculated imaginary frequency of 31i cm^{-1} and Pt−I distance of 4.501 Å in **16** seem to be similar to those for other iodide dissociation TSs studied here, **2**, **9**, and **11**. However, the activation energy associated with **16** is calculated to be only 12.3 kcal/mol, which is 5.3 kcal/mol less than that for TS **11**, 17.6 kcal/mol. In other words, having a σ-alkyl ligand in the *trans* position decreases the iodine dissociation barrier significantly. This is a well-known fact in many cases of σ-alkyl complexes of platinum.[85] Here, we demonstrated a similar behavior for σ-vinyl ligands. The dissociation process **6** → **17** is calculated to be exothermic by 38.2 kcal/mol.

In the next step, the second acetylene molecule coordinates to **17** to form a weak bound π-complex **18** with a complexation energy of only 2.6 kcal/mol. As seen in Figure 2, the Pt−C π-bond located *trans* to the vinyl ligand is about 0.32 Å longer than that located *cis* to the vinyl in **13**. Interestingly, complex **18** is found to be 9.4 kcal/mol more favorable than complex **13**. Starting from **18**, a nucleophilic addition to the coordinated triple bond proceeds via TS **19** and leads to *trans* divinyl complex **20**. Note, all three structures **18**−**20** were optimized assuming the C_s point group, where both organic ligands were placed in the same plane. Due to internal rotation of σ-vinyl and π-acetylene ligands, several isomers could be formed. However, taking into account the small energy barrier of internal rotation and the small energy difference between the possible isomers, here we have considered only one isomer presented in Figure 2 and discussed above.

TS **19** differs significantly from the TSs **5** and **14** discussed earlier. The forming C−I bond is significantly shorter, 3.093 Å in **19** compared with 4.052 Å in **5** and 4.356 Å in **14**. The difference in Pt−C breaking and forming bonds is 0.609 Å vs 0.161 Å in **14** and 0.250 Å

in **5**. In addition, the Mulliken charge on the attacking iodide is reduced by 15−20%. All the changes clearly show the more reactant-like nature of the TS **19**. The calculated energy barrier at TS **19** is 38.8 kcal/mol, which is 5.6 kcal/mol higher than that in the nucleophilic addition to structure **13**. The reaction **18** → **20** is calculated to be highly endothermic, 34.3 kcal/mol. Interestingly, the *cis* isomer of complex **20**, complex **15**, is calculated to be 8.6 kcal/mol lower in energy. This can be explained in terms of the destabilization effect of the two CH═CHI groups located *trans* to each other. An unusually long Pt−C distance, 2.143 Å, again confirms this conclusion.

Since the reverse reaction **20** → **18** has a barrier of only 4.4 kcal/mol, the formation of **20** is strongly unfavorable by both thermodynamic and kinetic factors and the structure most likely does not exist. The result is in agreement with experimental results, where only *cis*-divinyl derivatives were observed. Finally, one can conclude that neither path I nor path II may be a route to the desired product **15**, the former due to instability of **13** and the latter because of a higher activation barrier at TS **19**.

Note, as can be expected, the ZPCs have a very small effect on the activation energy of nucleophilic addition processes. However, its effect is significant on the acetylene binding process; the calculated ΔE + ZPC are −4.0 and −1.3 kcal/mol for complex **13** and **18**, respectively, compared to ΔE of −5.4 and −2.6 kcal/mol. Including entropy effects (see Table 2) reduces the I^- dissociation (**6** → **11** → **12** and **6** → **16** → **17**) barriers by 1 kcal/mol and makes the calculated processes 8.2−8.6 kcal/mol more exothermic. Meantime, inclusion of the entropy effects made the calculated barriers of the nucleophilic addition processes (**13** → **14** → **15** and **18** → **19** → **20**) larger by 5.7−7.0 kcal/mol, but the calculated energy of reaction 8.0−8.3 kcal/mol more endothermic. In other words, the Gibbs free energies make the iodide dissociation steps easier, but the π-complex formation and nucleophilic addition steps harder.

B. Effects of Solvent on the Reaction Mechanism. As shown above, the gas-phase studies adequately describe neither the first nor the second triple bond activation processes; calculated barriers are extremely high, which makes the reactions unfeasible, contrary to the experimental results. One of the reasons for this discrepancy could be the absence of the solvent effects in the gas-phase calculations. Indeed, in reality the present catalytic reaction proceeds either in water or in methanol solutions.[33,35,37] Therefore, in this section we will take into account the solvent effects using the PCM method. At first, we will study the reactions in the water environment. Later, we will extend our studies to the methanol environment, as well as to the solvent dependence of the key steps in a variety of solvents.

Dissociation of the Initial Pt^{IV} Iodide Complex and Acetylene Coordination. As seen in Table 2, inclusion of the water environment into calculations only slightly changes the iodine dissociation barrier for process **1** → **2**, increasing it from 18.1 to 20.5 kcal/mol. However, the energy of reaction **1** → **3** changed dramatically; in the gas phase it was exothermic by 30.3 kcal/mol, while PCM with the water solvent makes it endothermic by 13.4 kcal/mol. These changes could be explained in terms of weaker interaction of the polar water−solvent with the [PtI_5^- + I^-] system compared to the double-charged PtI_6^{2-} anion. As seen in Table 3, the electrostatic term makes a large contribution to the energy of solvation. Since the reactant **1** and TS **2** have very similar charges, the activation energy changed only slightly upon solvation. The same trends are observed for all I^- dissociation steps. As shown in Table 4, gas-phase calculations overestimate the stability of the dissociation products in solution by 38.8−43.7 kcal/mol, while the activation energy changes are within a few kcal/mol.

Table 3. PCM Solvation Energy Energies of Some Selected Compounds (in kcal/mol, solvent = water)

compound	total electrostatic term	total nonelectrostatic term	$\Delta G_{solvation}$
I^-	−62.09	−1.47	−63.56
PtI_5^-	−39.06	5.85	−33.22
PtI_6^{2-}	−144.78	6.27	−138.51

Table 4. Gas-Phase (ΔE_{gas}) and PCM Solution ($\Delta E_{solution}$) Energies of Reaction and Activation Energies of Iodide Ligand Dissociation Steps (in kcal/mol, solvent = water)

	energy of reaction			activation energy		
process	ΔE_{gas}	$\Delta E_{solution}$	$\Delta\Delta E$	$\Delta E^{\ddagger}_{gas}$	$\Delta E^{\ddagger}_{solution}$	$\Delta\Delta E^{\ddagger}$
1 → **3**	−30.3	13.4	43.7	18.1	20.5	2.4
8 → **10**	−41.9	−1.1	43.0	6.1	9.9	3.8
6 → **10**	−25.9	17.8	43.7	17.6	22.0	4.4
6 → **15**	−38.2	0.6	38.8	12.3	11.1	−1.2

Table 5. Gas-Phase (ΔE_{gas}) and PCM Solution ($\Delta E_{solution}$) Energies of Reaction and Activation Energies of Triple Bond Activation Steps (in kcal/mol, solvent = water)

	energy of reaction			activation energy		
process	ΔE_{gas}	$\Delta E_{solution}$	$\Delta\Delta E$	$\Delta E^{\ddagger}_{gas}$	$\Delta E^{\ddagger}_{solution}$	$\Delta\Delta E^{\ddagger}$
4 → **6**	19.2	−16.2	−35.4	34.3	5.1	−29.2
13 → **15**	15.9	−13.6	−29.5	33.2	9.1	−24.1
18 → **20**	34.4	4.8	−29.6	38.8	13.3	−25.5

As seen in Table 2, the solvent effect increases the acetylene binding energy in the π-complex **4** by only 0.5 kcal/mol, from 4.0 kcal/mol in the gas phase to 4.5 kcal/mol in the water−solvent. As shown in Table 5, in all the nucleophilic addition processes of the dissociated I^- to the coordinated acetylene, **4** → **6**, **13** → **15**, and **18** → **20**, the solvent effect dramatically changes both the activation barriers and the energies of reaction. The activation barriers were reduced by 24−30 kcal/mol, while the endothermicities of the reaction were decreased by 35.4−29.5 kcal/mol. As a result, the water−solvent effects make the nucleophilic addition to the coordinated triple C≡C bond a kinetically and thermodynamically feasible process. Specifically, PCM calculations result in the activation energy of 5.1 kcal/mol from π-complex **4** to TS **5**, an almost 7-fold reduction compared to the gas-phase value. The reaction becomes exothermic by 16.2 kcal/mol, making the formation of σ-vinyl compound **6** energetically favored. Solvent-corrected energetics are in line with experimental results, demonstrating that triple bond activation easily occurs at room temperature in water solution and leads to thermodynamically more stable σ-vinyl derivatives.

Now, let us discuss the solvent effects on the reaction **4** → **7** → **8**, an alternative acetylene activation mechanism corresponding to the insertion of the coordinated acetylene molecule into the Pt−I bond. According to above-presented gas-phase calculations, this reaction occurs with 8.5 kcal/mol barrier and is exothermic by 10 kcal/mol. As seen in Table 2, the water−solvent effect slightly reduces the barrier and exothermicity of the reaction to 7.2 and 9.6 kcal/mol, respectively. In the next steps, the coordination of the I^- ligand to the Pt-center in a position *trans* to the *Z*-CH=CHI group of **8** leads to the formation of octahedral complex **10** via TS **9**. The activation energy required for this step is calculated to be 10.2 kcal/mol in solution vs 53.0 kcal/mol in the gas phase, while process **8** → **9** → **10** is found to be endothermic by only 1.1 kcal/mol in water solution vs 41.8 kcal/mol in the gas phase. The entire reaction **4** → **10** in solution is calculated to be exothermic by 8.5 kcal/mol, while a similar process, **4** → **6**, leading to the *E*-isomer **6** is 16.2 kcal/mol exothermic.

To summarize, in solution the nucleophilic addition process is characterized by an activation barrier that is lower by 2.1 kcal/mol and leads to the formation of a product that is thermodynamically more stable by 7.7 kcal/mol than the insertion process. These results are consistent with available experimental results; the product of the insertion reaction, **10**, with *cis* orientation of Pt and I around the double bond, has never been observed.[33−37]

As seen in Table 2, entropy effects at 273 K ($\Delta G_{solution}$) do not change significantly the energetics of either the triple bond activation via Pt−I insertion (**4** → **7** → **8**) or the nucleophilic addition (**4** → **5** → **6**) mechanisms. $\Delta G_{solution}$ at the nucleophilic addition barrier (at TS **5**) is higher in energy than that at the insertion barrier (at TS **7**), in contrast to $\Delta E_{solution}$. However, the difference is only 1.7 kcal/mol, and both activation mechanisms may be operative under room-temperature conditions. Meanwhile, $\Delta G_{solution}$, in comparison with $\Delta E_{solution}$, for the first I^- dissociation step increases the activation energy by 3.2 kcal/mol and reduces the endothermicity of the reaction by 1.9 kcal/mol.

The Second Acetylene Molecule Activation. The second acetylene molecule activation proceeds via the same elementary steps, namely, iodide ligand dissociation, acetylene coordination, and nucleophilic addition to the coordinated triple bond. We have already discussed in detail the solvent effect on each of these steps; therefore only a brief description of PCM results on both path I and path II will be given here. The main attention will be focused on the factors controlling the formation of the *cis*-divinyl complex as a necessary precursor of the reductive C−C elimination reaction.

In path I starting from octahedral σ-vinyl compound **6**, a *cis*-iodide ligand dissociation occurs with an activation energy of 22.0 kcal/mol (4.4 kcal/mol higher than in the gas phase, see Table 4). The point of the reaction path corresponding to the unstable complex **12** with *cis* coordination vacancy lies about 12 kcal/mol higher compared to the reactant **6**. Taking into account the absence of isomerization barrier, this makes the formation of **12** very unfavorable. Mixed *cis*-{π,σ} complex **13** is 7.3 kcal/mol lower in energy than **12**. A relatively large acetylene binding energy reflects the larger instability of the precursor **12**. The second acetylene molecule activation in *cis* position to give a σ-vinyl ligand requires an activation energy of 9.1 kcal/mol, which is 24.1 kcal/mol smaller than the corresponding gas-phase value and 4.0 kcal/mol larger than the first iodoplatination step. The nucleophilic addition step, **13** → **14** → **15**, is calculated to be exothermic by 12.5 kcal/mol, which is close to the exothermicity of the first triple bond activation step (16.2 kcal/mol).

In path II, dissociation of *trans*-iodide ligand proceeds with an almost two times smaller activation barrier, 11.1 kcal/mol, due to the high *trans*-influence of the vinyl group, as discussed earlier. The formation of dissociation product **17** is endothermic by 0.6 kcal/mol. Subsequent acetylene coordination lowers the energy of the system by 1.7 kcal/mol, leading to weakly bound π-complex **18**. I^- attack to the coordinated triple bond after overcoming TS **19** with an activation barrier of 13.3 kcal/mol results in formation of the *trans*-divinyl complex **20**, which is 4.8 kcal/mol higher than reactants and 11.1 kcal/mol higher than corresponding *cis*-derivative **15**. Although solvation significantly changes the absolute values of the calculated energetics, the same relative trends in stability of final products and activation barriers are kept.

In contrast to gas-phase calculations, where the formation of **20** was strongly unfavorable both thermodynamically and kinetically, the solvent effects make this pathway feasible and worth pursuing. After iodide ligand dissociation through TS **21** with an activation energy of 22.3 kcal/mol, five-coordinated divinyl complex **22** of square pyramidal geometry is formed with an endothermicity of 15.2 kcal/mol. One may conclude that *trans* divinyl complexes are always thermodynamically unfavorable to *cis* derivatives. TS **23** corresponding to the *cis*−*trans* isomerization has been located, for which normal-mode analysis gives only one imaginary frequency of 21i cm^{-1}. It has a very early TS with ∠C−Pt−C = 167.6°, consistent with a very small activation energy of 0.1 kcal/mol in the gas phase (Table 2). In PCM calculations **23** is 0.8 kcal/mol lower in energy than the reactant **22**. Overcoming this TS leads to the five-coordinated *cis*-divinyl derivative **24**. This **20** → **24** rearrangement process is exothermic by 11.9 kcal/mol. Coordination of I^- to **24** results in the desired *cis*-$[Pt(CH=CHI)_2I_4]^{2-}$ complex. We did not locate the iodide ligand addition TS, since we have shown already that ligand addition/dissociation *trans* to the vinyl group proceeds rather easily (for example see **6** → **16** → **17** and reverse process).

Thus, complex **15**, which is a necessary initial compound for C−C reductive elimination reaction and has two *cis*-positioned carbon atoms, can be obtained after a second acetylene molecule activation (**18** → **19** → **20**) and subsequent isomerization (**20** → **21** → **22** → **23** → **24** → **15**). Although the formation of compound **20** from the π-complex **18** is an endothermic process, the final product **15** is thermodynamically favored. The rate-determining step of this process is **20** → **22**, which occurs with a 22.3 kcal/mol barrier. Therefore, one may conclude that, in solution, **15** can be formed at the room temperature with the proposed mechanism, but the reaction would be slow. Finally, we can conclude that path II seems to be the most likely pathway in solution

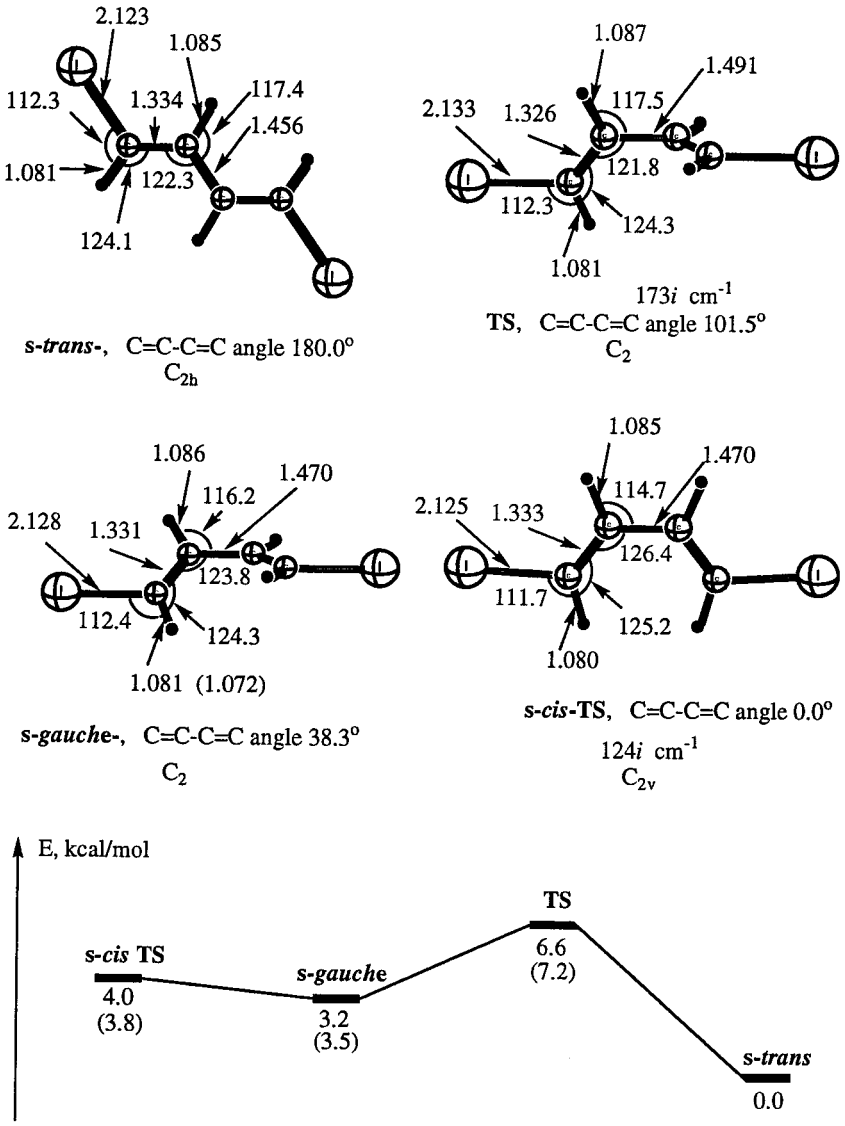

Figure 4. *E*,*E*-1,4-Diiodobuta-1,3-diene conformations. Selected geometry parameters are given in Å and deg; energy in parentheses corresponds to PCM calculations in water.

for the second acetylene molecule activation process leading to *cis*-divinyl complex as a final product. Path I is unlikely to take place in solution.

A comparison of $\Delta E_{solution}$ and $\Delta G_{solution}$ given in Table 2 shows the following main features. For all I^- dissociation steps (**6** → **11** → **12**, **6** → **16** → **17**, and **20** → **21** → **22**) the activation barrier using $\Delta G_{solution}$ is about 3.0−3.7 kcal/mol higher than that with $\Delta E_{solution}$. All these steps are 2.3−2.6 kcal/mol more exothermic with $\Delta G_{solution}$ than with $\Delta E_{solution}$. The energetics of the π-complex formation process (**12** → **13** and **17** → **18**) are almost the same at the $\Delta E_{solution}$ and $\Delta G_{solution}$ levels. As to the energetics for nucleophilic addition steps (**13** → **14** → **15** and **18** → **19** → **20**), $\Delta G^{\ddagger}_{solution}$ and $\Delta G_{solution}$ are 2.2−4.1 kcal/mol higher than corresponding $\Delta E^{\ddagger}_{solution}$ and $\Delta E_{solution}$, respectively. Also, it should be noted that $\Delta G^{\ddagger}_{solution}$ energies for all steps of the second acetylene molecule activation are higher than their corresponding $\Delta E^{\ddagger}_{solution}$ values. However, these differences are only 1−2 kcal/mol; therefore, in Figure 3 we have presented the potential energy surfaces of these reactions using only calculated $\Delta G_{solution}$ values in aqueous solution.

4. Vinyl−Vinyl Reductive Coupling on Pt^{IV} Complexes

Direct C−C reductive elimination reactions are well known in the literature. For example, a three-centered C(sp)−C(sp^2) reductive elimination from Pt^{II} complexes was proposed based on the activation parameters.[40] Theoretical studies[44−48] of ethane formation [C(sp^3)−C(sp^3) reductive elimination] from methylplatinum complexes found a three-centered TS for a C−C σ-complex formation. The reductive vinyl−vinyl coupling from divinyl derivative **15** gives *E*,*E*-1,4-diiodobuta-1,3-diene, as proved experimentally.[33,35,37] However, it is well known that 1,3-dienes usually possess few conformations due to rotation around the middle C−C bond. To the best of our knowledge there were no theoretical calculations or experimental data published on the C(sp^2)−C(sp^2) reductive elimination from divinyl Pt complexes. In the present work we have performed a comprehensive conformational search in order to address this question.

Optimized structures and selected geometry parameters of the reactants, TSs, and products are shown in

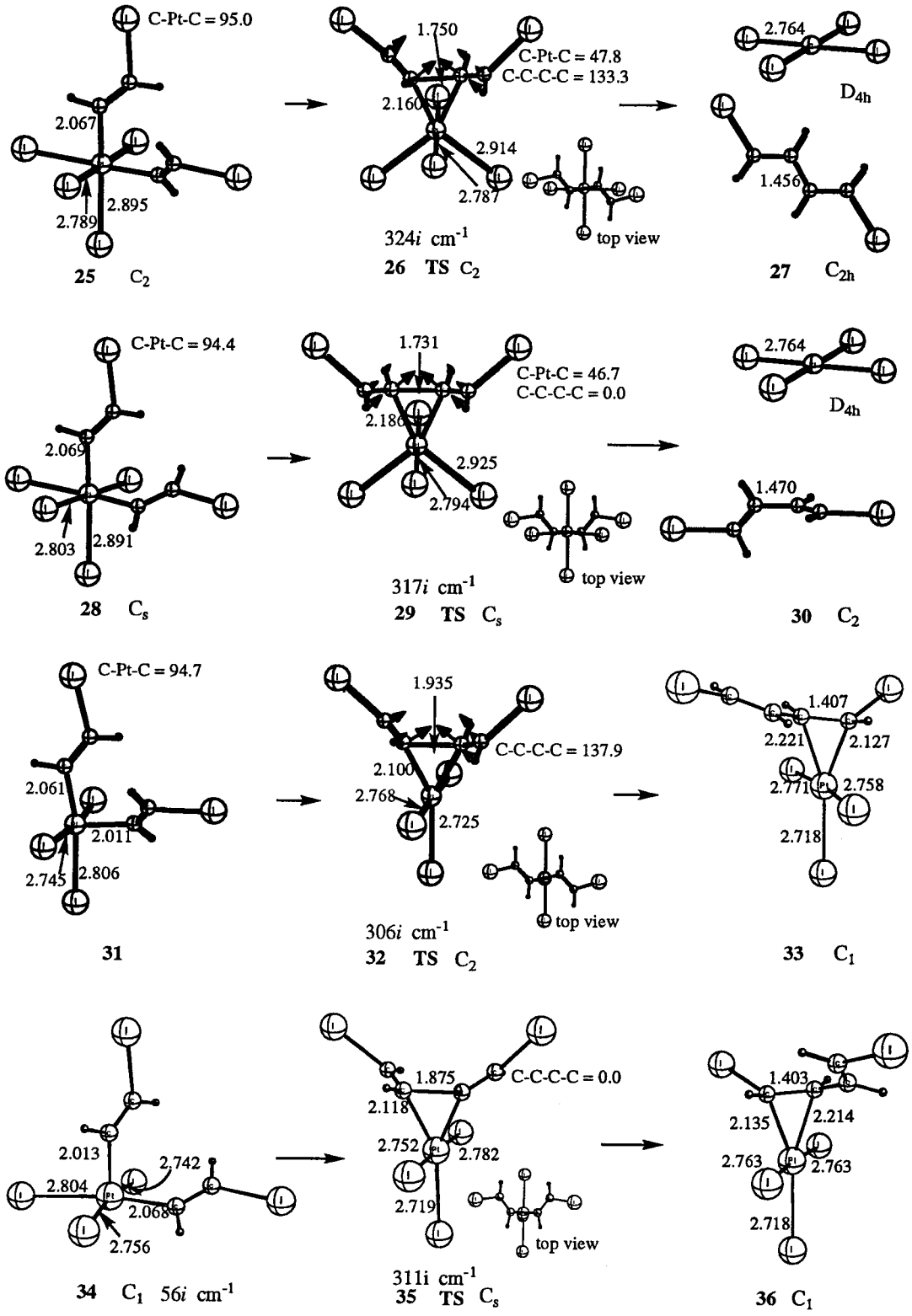

Figure 5. *s-cis* and *s-trans* reductive elimination pathways from divinyl complexes. Some selected geometry parameters are given in Å and deg.

Figures 4 and 5. Their relative energies are summarized in Table 2. Below, we will study the gas-phase reactions and will discuss the solvent effects. In both cases, we will study the vinyl−vinyl reductive coupling reactions of both six- and five-coordinated complexes.

A. Gas-Phase Calculations. The most stable form of the product of this reaction, *E*,*E*-1,4-diiodobuta-1,3-diene, is an *s-trans* isomer. This isomer could be converted to the another isomer, *s-gauche*, which lies 3.2 kcal/mol higher in energy, with a 6.6kcal/mol barrier, as shown in Figure 4. The *s-cis* TS, with the only imaginary frequency of 124i cm^{-1}, connects an *s-gauche* form (C=C−C=C angle 38.3°) with another (−38.3°) with a small barrier of 0.8 kcal/mol. The longest C−C bond of 1.491 Å is found in the TS connecting *s-trans* and *s-gauche* isomers. The shortest C−C bond of 1.456 Å is found in the most stable *s-trans* form. The calculated relative energies of *E*,*E*-1,4-diiodobuta-1,3-diene

are very close to those reported in the literature for unsubstituted buta-1,3-diene: 0.0, 5.2, 2.4, 3.6 kcal/mol for *s-trans*, TS, *s-gauche*, and *s-cis* structures, respectively, calculated at the MP3/6-311++G**//MP2/6−31* level.[86]

Reductive Coupling from the Six-Coordinated Complexes. Our extensive search has shown that C−C bond formation between vinyl ligands on the six-coordinate complex *cis*-$(ICH{=}CH)_2PtI_4$ proceeds through two different TSs leading to the formation of *s-trans* and *s-cis* butadiene isomers, respectively. The reactants and products to which these TSs are connected were confirmed by the IRC. As seen in Figure 5, the reaction from an initial complex **25** involves TS **26** (324i cm^{-1}) leading to an *s-trans* isomer. Moving along the reaction coordinate maintaining C_2 symmetry, the C−Pt−C angle is decreased from 95.0° in initial complex **25** to 47.8° in TS **26** and the Pt−C bond length is increased by 0.093 Å. The C−C distance is found to be 1.750 Å in TS **26**. Pt−I bonds do not change significantly; the largest deviation is within 0.02 Å. Upon dissociation of *s-trans-E,E*-1,4-diiodobuta-1,3-diene, the iodide ligands, located in *trans* positions to CH=CHI groups in **25**, move into the equatorial plane, giving a square planar PtI_4^{2-} complex. The reductive elimination barrier at TS **26** is calculated to be 28.0 kcal/mol, and the process **25** → **26** → **27** leading to *s-trans-E,E*-1,4-diiodobuta-1,3-diene is found to be exothermic by 6.5 kcal/mol.

C−C bond formation can also start from complex **28**, which is an isomer of **25**, and proceed, maintaining the C_s symmetry, through alternative TS **29** to lead to the *s-gauche* conformer of the butadiene molecule. Final products **30** of this reductive elimination process are *s-gauche-E,E*-1,4-diiodobuta-1,3-diene and square planar PtI_4^{2-}. The structure of TS **29** is very similar to that of **26** discussed above, however with more late character. The C−Pt−C angle is smaller (46.7° in **29** vs 47.8° in **26**), while Pt−C bonds are longer (2.186 Å in **29** vs 2.160 Å in **26**). In agreement with more product-like TS, the reductive elimination barrier at **29** is increased to 31.4 kcal/mol and the exothermicity of the process **28** → **29** → **30** is reduced to 5.0 kcal/mol, compared with those for the process **25** → **26** → **27**.

Since (i) isomer **28** is energetically 1−2 kcal/mol less stable than isomer **25** and (ii) separated from the latter by a small (expected to be about 1−2 kcal/mol) rotational barrier and (iii) the barrier at transition state **29** is significant, one may expect the process **28** → **29** → **30** to be unfeasible. Instead, complex **28** at first will rearrange into **25**, and reaction will proceed via the path **25** → **26** → **27**, leading to the *s-trans* product. In other words, the product of the reductive elimination process is always going to be an *s-trans* conformer, which is consistent with the experiment. Although the *s-trans* conformation was assigned to be the final product in the experimental study, this information cannot be used to distinguish the mechanisms of reductive elimination since the conformers, *s-trans* and *s-gauche*, are separated with a rather low energy barrier.

Reductive Coupling from Five-Coordinated Complexes. We have found that dissociation of iodide ligand in *trans* position to the σ-vinyl group requires a small activation energy of about 11 kcal/mol (see **16**). Taking this into account, we have studied the C−C reductive elimination process from the five-coordinated Pt^{IV} divinyl complex.

The structures of initial complex, TS, and products of the vinyl−vinyl reductive elimination process through an *s-trans* mechanism are shown in Figure 5. Initial complex **31** has square pyramidal geometry with slightly different Pt−C bond lengths, 2.061 and 2.011 Å, where the latter one is rather short due to the absence of a ligand in *trans* position. TS structure **32** significantly differs from **26** located for octahedral geometry. Pt−C bond lengths in **32** are significantly shorter than in **26**, 2.100 and 2.160 Å, correspondingly, while the C−C distance is longer, 1.935 vs 1.750 Å. Normal-mode analysis for **32** gives only one imaginary frequency of 306i cm^{-1}, which represents the reaction path. Comparing TSs **32** and **26**, one may conclude that the former has an earlier character, which is consistent with the obtained smaller activation energy, 7.8 kcal/mol, for the former. Overcoming TS **32** leads to structure **33**. The geometry of **33** corresponds to a typical π-complex of Pt(II) with a C=C double bond. Ligand exchange reaction with iodide gives PtI_4^{2-} and *E,E*-1,4-diiodobuta-1,3-diene as final products (the same products as **27**).

The structures of TS (**35**), product (**36**), and the nearly converged structure of initial complex (**34**) for the C−C elimination process through the s-*cis* mechanism are also shown in Figure 5. The imaginary frequency of 56i cm^{-1} for **34** corresponds to internal rotation of vinyl ligands around Pt−C bonds. Since internal rotation only slightly changes the energy (see subsection 3.A) and is unlikely to have serious effect on our final conclusions, we did not fully optimize the geometry. Note, **34** has square pyramidal geometry with the longer Pt−C bond opposite the iodide ligand (2.068 vs 2.013 Å). As in the cases of **32** and **26**, comparing TS structures **35** and **29** shows that the former has more reactant-like character; Pt−C bonds are shorter, 2.118 in **35** vs 2.186 Å in **29**, while the C−C bond lengths are 1.875 Å in **35** and 1.731 Å in **29**. The calculated activation barrier, 9.4 kcal/mol, at TS **35** is much smaller than for the analogous process involving six-coordinated complexes, 31.4 kcal/mol at the **29**.

Upon comparing TSs **32** and **35**, one finds the same relative trends as those for **26** and **29**. Reductive elimination via the *s-cis* mechanism results in more product-like TSs and higher activation energies, by 3.4 and 1.6 kcal/mol for six- and five-coordinated complexes, respectively. The difference in energy is close to that for the products, *trans*- and *cis-E,E*-1,4-diiodobuta-1,3-diene, 4.0 kcal/mol, as seen in Figure 4. Therefore, the difference in the strain energy in the butadiene unit is the likely origin of the relative stability of the two TSs.

The ZPC does not change significantly the activation barriers (less than 1 kcal/mol) or the reaction energies (all reactions becoming more exothermic by 1.2−2.3 kcal/mol) of the C−C reductive coupling reactions for six- or five coordinated complexes. Meanwhile, the entropy effect in ΔG reduces the diiodobutadiene dissociation energy by 10.8−11.4 kcal/mol compared to ΔE values, but does not change the relative energies of the other structures significantly (only 0.4−3.1 kcal/mol).

(86) Wiberg, K. B.; Rablen, P. R.; Marquez, M. *J. Am. Chem. Soc.* **1992**, *114*, 8654.

B. Effects of Solvent on the Reaction Mechanism. Reductive Elimination from Six-Coordinated Complexes. As shown in Table 2, the PCM solvent effects reduce the barriers for reductive C−C coupling reactions for the octahedral divinyl complexes to 20.1 and 25.5 kcal/mol for *s-trans* and *s-cis* mechanisms, respectively, from their gas-phase values of 28.0 and 31.4 kcal/mol. Although both barriers are decreased, the same relative order is maintained; the formation of the *s-trans* configuration of butadiene is kinetically more preferable. Meanwhile, the PCM calculations increase the exothermicity of the processes **25** → **27** and **28** → **30** dramatically from 6.5 and 5.0 kcal/mol to 32.3 and 29.3 kcal/mol, respectively.

Reductive Elimination from Five-Coordinated Complexes. The PCM solvent effects in the C−C reductive elimination reaction from the five-coordinated complexes reproduce the same trends as found for the six-coordinated species discussed above. Activation energies of the processes **31** → **32** → **33** and **34** → **35** → **36** decrease slightly from the gas-phase values of 7.8 and 9.4 kcal/mol to 7.0 and 6.6 kcal/mol, while the exothermicities increase slightly from 31.1 and 29.1 kcal/mol in the gas phase to 34.9 and 33.4 kcal/mol, respectively.

One should note that, in general, the total free energy of solvation $\Delta G_{solution}$ in Table 2 does not differ significantly from the $\Delta E_{solution}$. The same is applicable for all reductive elimination reactions; the difference between $\Delta G^{\ddagger}$ and $\Delta E^{\ddagger}$ is within 1 kcal/mol and between ΔG and ΔE within 0.6−4.3 kcal/mol.

5. Solvent Dependence of Energetics

In the above sections, we have discussed the PCM results obtained for the acetylene activation in water solution. However, under experimental conditions the catalytic acetylene triple bond activation may proceed either in water or in methanol solutions;[35,37] synthesis of 1,4-diiodobuta-1,3-diene is reported in methanol[35] and catalytic conversion of substituted alkyne ($HC{\equiv}C{-}CH_2{-}OH$) in water.[33] The above-presented calculations have shown the critical importance of the solvent effect on the energetics of the catalytic cycle. Therefore, it is very important to address the question of solvent dependence of this reaction in more detail. In Table 6, we have presented the PCM results in water, methanol, acetone, benzene, chloroform, and the gas phase for the five most important steps such as (1) I^- ligand dissociation, (2) triple bond activation via external nucleophilic addition, (3) triple bond activation via insertion reaction, (4) C−C reductive coupling from six-coordinated octahedral complex (*s-trans* mechanism only), and (5) C−C reductive coupling from five-coordinated square pyramidal complex (*s-trans* mechanism only). (The PCM relative energies for some selective intermediates and transition states are presented in Table S1 in the Supporting Information.)

As seen in Table 6, the activation free energy ($\Delta G^{\ddagger}$) of the acetylene triple bond activation via external nucleophilic addition strongly depends on the solvent polarity and changes from 39.9 kcal/mol in the gas phase ($\epsilon = 1.0$) to 9.3 kcal/mol in water ($\epsilon = 78.4$). Its reaction free energy also strongly depends on the nature of solvent, changing from endothermic in the gas phase ($\Delta G = 27.6$ kcal/mol) to exothermic in water solutions ($\Delta G = -13.1$ kcal/mol). Unambiguously, the reaction is kinetically and thermodynamically favored in more polar solvents. For the acetylene triple bond activation via insertion, the energetics of the reaction is almost unaffected by the polarity of the media. Both $\Delta G^{\ddagger}$ and ΔG change within 1 kcal/mol in all solvents and in the gas phase.

Table 6. Activation and Reaction Free Energies ($\Delta G^{\ddagger}$ and ΔG) of Some Selected Steps Calculated at the PCM Level in Different Solvents and Gas Phase, Where ϵ Denotes Dielectric Constant (Negative ΔG Corresponds to Exothermic Process)

	water $\epsilon = 78.4$	methanol $\epsilon = 32.6$	acetone $\epsilon = 20.7$	chloroform $\epsilon = 4.9$	benzene $\epsilon = 2.2$	gas phase $\epsilon = 1.0$
I^- Dissociation: **1** → **2**(TS) → **3**						
$\Delta G^{\ddagger}$	23.7	22.8	23.8	23.5	22.8	17.7
ΔG	11.5	9.8	7.8	0.9	−9.4	−38.0
Nucleophilic Addition: **4** → **5**(TS) → **6**						
$\Delta G^{\ddagger}$	9.3	9.5	9.9	14.8	21.8	39.9
ΔG	−13.1	−12.3	−11.5	−5.5	3.0	27.6
Insertion Reaction: **4** → **7**(TS) → **8**						
$\Delta G^{\ddagger}$	7.6	7.5	7.6	8.0	8.3	7.9
ΔG	−9.4	−9.6	−8.8	−9.0	−9.4	−9.8
C−C Elimination (6-coordinated): **25** → **26**(TS) → **27**						
$\Delta G^{\ddagger}$	20.7	20.8	21.9	26.6	27.4	27.6
ΔG	−36.7	−36.1	−36.0	−28.6	−23.3	−17.3
C−C Elimination (5-coordinated): **31** → **32**(TS) → **33**						
$\Delta G^{\ddagger}$	6.3	6.6	6.8	7.0	7.0	9.2
ΔG	−35.9	−35.4	−34.6	−33.9	−33.2	−28.0

The ΔG of the iodide ligand dissociation reaction is strongly influenced by solvent, 11.5 kcal/mol in water and −38.0 kcal/mol in the gas phase. However, the corresponding barrier depends relatively less (changes are about 7 kcal/mol) on the nature of the solvent. It is interesting to note that, in contrast to the previous process, the dissociation reaction becomes kinetically and thermodynamically unfavorable in polar solvents.

The vinyl−vinyl reductive elimination reaction from the six-coordinated octahedral complex is characterized by a medium solvent effect on $\Delta G^{\ddagger}$ and a strong one on ΔG. The same reaction from five-coordinated square pyramidal compounds shows small and medium solvent effects on $\Delta G^{\ddagger}$ and ΔG, respectively. Reductive elimination from both types of complexes is favored in polar solvents for both thermodynamic and kinetic reasons.

Thus, summarizing the results for all individual steps, one may conclude that (1) more polar solvents (water, methanol) significantly facilitate catalytic acetylene conversion into diidosubstituted diene; (2) both insertion and nucleophilic addition processes may take place in solvents with a relatively large dielectric constant, like water, methanol, or acetone. However, the insertion process is preferable in the media with smaller ϵ values, chloroform or, especially, benzene; (3) one may be able to control the direction of the activation process and, as a result, stereoselectivity of the reaction by changing the polarity of the media.

6. Discussions and Conclusions

We have presented the first computational study of the catalytic cycle of acetylene triple bond activation by Pt^{IV} iodide complexes and subsequent vinyl−vinyl coupling leading to conjugated butadiene products. The following important features of the present system may be worth discussing.

1. Our calculations demonstrated the importance of the solvent effect on the entire catalytic cycle. According to gas-phase calculations, (i) the acetylene triple bond activation through the insertion mechanism (**4** → **7** → **8**) is energetically more favorable to nucleophilic addition (**4** → **5** → **6**), and (ii) the second acetylene molecule activation does not lead to a stable divinyl complex. However, the solvent effects correct these results and make them consistent with the experiment.

It was shown that in water solution the acetylene triple bond activation by Pt^{IV} iodide complexes should proceed easily via the nucleophilic addition mechanism with a relatively low activation barrier and high exothermicity ($\Delta G^{\ddagger} = 9.3$ kcal/mol and $\Delta G = -13.1$ kcal/mol for **4** → **5** → **6**). The triple bond activation via the insertion mechanism (**4** → **7** → **8** → **9** → **10**) may also take place because of a similar low activation barrier. However, the product **10** with a *Z*-substituted vinyl ligand is thermodynamically 7.1 kcal/mol unfavorable compared to **6**, where the *E*-substituted vinyl ligand is formed as a result of external nucleophilic addition. In general, the gas-phase results mimic the solution results only for the step where the reactant and the product have similar charge distribution and the solvent effect is similar.

On the basis of the above-presented energy difference between the complexes **10** and **6** with *Z*-substituted and *E*-substituted vinyl ligands, respectively, one expects that the difference in thermodynamic stability of divinyl complexes with two *Z*- and *E*-substituted vinyl ligands will be approximately twice the value obtained for monovinyl derivatives. Therefore, the final *Z*,*Z*-1,4-diiodobuta-1,3-diene product may not be formed due to thermodynamic instability of the corresponding divinyl complex with two *Z*-substituted vinyl ligands. These findings are in good agreement with experimental observation,[33−37] where only the *E*,*E*-type diene product was detected.

2. Calculated instability of compound **12** clearly shows the inadequacy of the previously proposed mechanism[33,35] of the second acetylene molecule activation leading to *cis*-divinyl derivative **15**. According to our calculations, this process most probably involves the formation of *trans*-divinyl complex **20**, followed by isomerization to the thermodynamically more stable *cis* derivative **24**, and the recoordination of the iodine anion. The barrier, $\Delta G^{\ddagger} = 25.6$ kcal/mol, of the **20** → **21** isomerization reaction is found to be the rate-determining step of the entire process. Although the barrier is significant, the reaction **20** → **24** is thermodynamically favored by 14.1 kcal/mol. These results are in excellent agreement with experimental findings,[33−37] since only the slow formation of *cis*-divinyl complexes was observed.

3. Detailed examination of possible C−C reductive coupling reaction mechanisms resulted in finding two alternative pathways proceeding from the six- and five-coordinated platinum complexes, respectively, among which the latter is slightly more favorable. It was shown that vinyl−vinyl coupling proceeds with a small (7.0 kcal/mol) activation barrier and leads to the *s-trans* butadiene product. However, a larger activation energy was found in the case of six-coordinated complexes (20.1 kcal/mol).

The results are in excellent agreement with available experimental and theoretical results[26,87] for reductive elimination from similar dimethyl complexes of Pt^{IV}. Namely, it has been shown that decomposition of five-coordinated compounds proceeds much faster, and the C−C reductive elimination at room temperature starts only after dissociation of one of the ligands from the octahedral complex.[88] Recently, it has been also shown that five-coordinated complexes play a very important role in C−C, C−I, C−O reductive elimination reactions from octahedral Pt^{IV} complexes.[88−91]

Thus, we have found that the free energy surface constructed at the B3LYP-PCM level provides a reasonable description of the potential surface for the present catalytic system in solution. The catalytic reaction starts with the acetylene triple bond activation via external nucleophilic addition. The second acetylene molecule activation occurs in *trans* position to the present vinyl ligand, followed by isomerization to the *cis*-divinyl derivative, which is found to be a rate-determining step of the catalytic cycle. The final butadiene product is formed through the reductive C−C coupling reaction, preferably from the five-coordinated intermediate. To the best of our knowledge, this paper represents the first theoretical investigation of vinyl−vinyl coupling reaction and triple bond activation by transition metal iodide complexes. The calculated results are in a very good agreement with available experimental findings and afford quantitative description of the entire catalytic cycle.

Acknowledgment. The present research is in part supported by a grant (CHE-9627775) from the National Science Foundation. Acknowledgment is also made for generous support of computing time at Emerson Center of Emory University and the U.S. National Center for Supercomputing Applications (NCSA).

Supporting Information Available: (a) The optimized Cartesian coordinates of all reactants, transition states, and products of the reactions presented in this paper, (b) Figure S1 including rotational transition states for structures **4**, **10**, and **6**, (c) Scheme S1 schematically representing the π-complex **4** and transition state **5**, and (d) Table S1 including PCM solution energy ($\Delta E_{solution}$) and free energy ($\Delta G_{solution}$) of some selected structures of the above-presented reaction in different solvents.

OM001073U

(87) (a) Crumpton, D. M.; Goldberg, K. I. *J. Am. Chem. Soc.* **2000**, *122*, 962. (b) Bartlett, K. L.; Goldberg, K. I.; Borden, W. T. *J. Am. Chem. Soc.* **2000**, *122*, 1456.
(88) Hill, G. S.; Yap, G. P. A.; Puddephatt, R. J. *Organometallics* **1999**, *18*, 1408.
(89) Williams, B. S.; Holland, A. W.; Goldberg, K. I. *J. Am. Chem. Soc.* **1999**, *121*, 252.
(90) Goldberg, K. I.; Yan, J. Y.; Breitung, E. M. *J. Am. Chem. Soc.* **1995**, *117*, 6889.
(91) Goldberg, K. I.; Yan, J. Y.; Winter, E. L. *J. Am. Chem. Soc.* **1994**, *116*, 1573.
(92) Sadlej, A. J. *Theor. Chim. Acta* **1992**, *81*, 339.